SUPPLEMENTARY INFORMATION (SI) APPENDIX FOR

Costs and benefits of provocation in bacterial warfare

Diego Gonzalez[b,c,1], Akshay Sabnis[a], Kevin R. Foster[b], Despoina A.I. Mavridou[a,1]

[a]MRC Centre for Molecular Bacteriology and Infection, Department of Life Sciences, Imperial College London, Kensington, London, SW7 2DD, UK; [b]Department of Zoology, University of Oxford, Oxford, OX1 3PS, UK; [c]Department of Fundamental Microbiology, Faculty of Biology and Medicine, University of Lausanne, 1015 Lausanne, Switzerland

[1]To whom correspondence should be addressed. D.A.I. Mavridou, MRC Centre for Molecular Bacteriology and Infection, Department of Life Sciences, Imperial College London, Kensington, London, SW7 2DD, UK, Tel: +44(0)2075949936 E-mail: d.mavridou@imperial.ac.uk; D. Gonzalez, Department of Fundamental Microbiology, Faculty of Biology and Medicine, University of Lausanne, 1015 Lausanne, Switzerland, E-mail: diego.gonzalez@unil.ch.

This PDF file includes:

SUPPLEMENTARY INFORMATION MATERIALS AND METHODS

ODE model. We modeled the dynamics of toxin-secreting cell populations using systems of Ordinary Differential Equations (ODE). For simplicity, we assumed a well-mixed environment with limited nutrients (batch culture). Different strains, which produce either no toxin (sensitive strains) or one type of toxin (toxin-producing strains), coexist in this environment. All strains have the same probability of lysing per generation and when they do, and provided they are toxin-producing strains, they produce the same number of toxin molecules. The substrate consumption, the population dynamics of each strain, and the dynamics of molecules of each type of toxin are modeled by distinct equations.

The substrate consumption is given by the following equation, classically derived from Monod's function (1, 2):

$$\frac{dS}{dt} = -\frac{1}{\gamma} N \frac{rS}{a + S}$$

where S is the amount of substrate, N the number of cells in the whole population, r the maximum growth rate, a the half-saturation constant, and γ the growth yield.

For the population dynamics of each strain we considered the rate of spontaneous lysis and the extrinsic death due to the toxins produced by each competitor. The probability of extrinsic death is assumed to be proportional to the product of the strain population and the number of free toxin molecules produced by other strains (3). The strain equation, therefore, is:

$$\frac{dN_i}{dt} = N_i \frac{rS}{a + S} - N_i \left(l + \sum_{x=j, x \neq i}^{n} T_x p_{ix} \right)$$

where N_i is the population of strain i, l the spontaneous cell lysis rate, T_x the number of molecules of toxin x produced by strain x, and p_{ix} a constant representing the probability for a cell of strain N_i to be killed by a molecule of toxin x. Sensitive strains which produce no toxin are assumed to lyse at the same rate as toxin-producing strains. The value of p_{ix} is assumed to be the same for all strain-toxin pairs, except for resistant strains, for which p_{ix}=0 for all toxins.

The number of free toxin molecules is given by the sum of the molecules produced by spontaneous and retaliation-driven lysis minus decay:

$$\frac{dT_i}{dt} = N_i h \left(l + \sum_{x=j, x \neq i}^{n} T_x k_x p_{ix} \right) - dT_i$$

where T_i is the number of molecules of toxin i produced by strain i, h the number of toxin molecules produced per cell lysis event, d the toxin-inactivation rate and k_x a factor associated with every toxin which defines whether it is an aggression-provoking toxin (k_x=1) or not (k_x=0). Aggression-provoking toxins behave exactly like all other toxins, except for the fact that the competitor cells they kill produce toxins before dying; the number of toxin molecules produced per killed cell (h) is the same as during spontaneous lysis. Since, in

accordance with the literature, a single molecule of toxin is sufficient to kill a target cell (4), aggression-provoking toxins do not increase the rate of spontaneous lysis (*l*) of competing populations, which means that they only trigger toxin production in cells which are doomed to die. We have confirmed this in our experimental system (see Fig. S27).

To model scenarios where three strains compete, but one focal strain is partially protected from toxins secreted by the other two, we increased the probability for the two competitors to reach each other with their toxins by multiplying the constant p_{ij} by a variable positive integer *u* (which we term segregation factor).

Variables and parameters of the model are stated bellow.

State variables	**Description**	**Initial Value**
S	substrate amount	$8*10^{-3}$
N	number of bacteria within a strain population	10^5
T	number of toxin molecules produced by a strain	0

Parameters	**Description**	**Value**
p_{ij}	probability for a cell *i* to be killed by toxin *j* (per cell-toxin encounter); for resistant strain, $p_{ij} = 0$	0 or $4*10^{-12}$
k_j	provocation status of toxin *j;* for provoking toxin, $k_j = 1$	0 or 1
r	maximal growth rate	1.35
a	half-saturation constant	4*10-3
γ	growth yield	$2.4*10^{11}$
l	lysis rate	0.01
h	number of toxin molecules per lysis event (5)	10^5
u	segregation factor	1 to 20
f	growth rate bias for the focal strain (for segregation scenario)	1 to 2

The simulations were carried out using R (http://www.R-project.org). The *deSolve* library (6) was used to solve ODEs, and relative fitness was calculated as the population change of each strain relative to the fittest strain in presence for each pair of consecutive time points.

Spatial model. To include the impact of spatial structure in our theoretical predictions, we implemented the model described in Fig. S3 using the *igraph* package in R (http://www.R-project.org). We chose a 20x20 toroidal lattice graph, with vertices that can be occupied by, at most, one cell at a time and by any number of different toxin types. Each simulation run comprised 40 cycles. The overall and single-strain occupancy of the lattice was recorded at the end of each cycle. Simulation runs were repeated 40 times for each condition. Averages and 97.5% confidence intervals are presented in the graphs.

Meta-community model. We simulated the evolution of populations of sensitive and resistant non-producers in co-existence with sensitive and resistant toxin producers. These strains compete for individual niches according to the following intuitive rules: 1. Sensitive non-producers outcompete resistant non-producers; 2. Resistant non-producers outcompete both sensitive and resistant toxin producers; 3. Sensitive toxin producers outcompete sensitive non-producers; 4. Resistant toxin producers outcompete sensitive toxin producers; 5. When

two sensitive or two resistant toxin producers meet, the strain that dominates is selected at random. We used a model comprising 1,600 niches. During the initial cycle, each niche was assigned at random two (or three) strains which compete for dominance. During the following cycles, each niche was assigned two (or three) strains randomly selected from the pool of 1,600 winners of the previous cycle along with one of the initial strain types; by always including one of each of the initial strain types, we assumed a low (< 0.1%) migration rate to avoid extinctions. The frequency of each strain within the system was recorded at the end of each cycle for 100 cycles. We note that this model is not intended to provide an accurate account of the evolution of natural colicinogenic communities. Nonetheless, it illustrates well the periodic dominance and coexistence of strains, also predicted in other more realistic or spatial models that have been developed and tested elsewhere (7, 8).

Bioinformatics. The following bioinformatics analyses were performed in this study. Scripts and pipelines were written in perl (version 5.18.2) and executed on macOS Sierra 10.12.5.

FijiCOMP data (http://fijicomp.bme.cornell.edu)

We searched between 3 and 3.5 Gbases of reads extracted from each FijiCOMP individual stool microbiome database for the presence of colicin encoding genes using tblastn_vdb (SRA toolkit 2.8.2) (https://www.ncbi.nlm.nih.gov/sra/docs/toolkitsoft/) with e-value < 10. Queries included (NCBI gi number): Alveicin_A (499491735), Cloacin_DF13 (10955256), Colicin_5 (1212893), Colicin_10 (807876), Colicin_A (9507292), Colicin_B (727400684), Colicin_D (695196167), Colicin_E1 (9507254), Colicin_E2 (204309820), Colicin_E3 (695196661), Colicin_E4 (754716641), Colicin_E5 (587677783), Colicin_E6 (144395), Colicin_E7 (144375), Colicin_E8 (242347932), Colicin_E9 (222098967), Colicin_FY Colicin_FY (410688433), Colicin_Ia (695197212), Colicin_Ib (9507452), Colicin_K (61965912), Colicin_M (169546453), Colicin_N (748133257), Colicin_R (542675452), Colicin_S4 (5295807), Colicin_U (695198141), Colicin_V (84060908), Colicin_Y (10955435), Klebicin_B (11342751). Datasets (experiments) included: SRS475534, -537, -539, -540, -541, -542, -545, -546, -549, -565, -566, -567, -568, -572, -575, -578, -585, -586, -589, -594, -598, -604, -611, -612, -613, -621, -624, -625, -626, -627, -630, -631, -648, -651, -658, -662, -664, -666, -667, -673, -681, -682, -684, -689, -690, -692, -694, -695, -698, -701, -702, -703, -705, -709, -722, -723, -920, -924, -925, -929, -931, -933, -936, -944, -953, -958, -962, -967, -968, -979, -980, -981, -984, -986, -987, -989, -990, -993, -994, -997, -998, SRS476001, -013, -014, -015, -019, -020, -021, -034, -035, -037, -050, -051, -058, -070, -076, -077, -083, -092, -094, -095, -096, -097, -098, -100, -101, -^{103}, -104, -106, -108, -114, -119, -120, -121, -125, -128, -139, -141, -142, -143, -144, -147, -148, -153, -154, -155, -159, -160, -163, -164, -166, -167, -169, -173, -182, -183, -184, -185, -187, -188, -189, -191, -192, -195, -198, -205, -211, -213, -262, -267, -269, -270, -271, -273, -274, -276, -277, -278, -280, -287, -290, -291, -293, -295, -296, -302, -306, -326, -328, -342, -430, -489, -518, -519, -794, SRS477428. Aligned reads longer than 59 bp and with more than 95% identity to a query were considered matches to the colicin gene with the highest percent identity. A colicin gene was considered present in a microbiome if at least three reads aligned with its protein sequence with more than 95% identity and if more than 15% of the colicin sequence length was covered. The list of datasets and the results of the analysis can be found in Dataset S2.

Human Microbiome Project data (https://www.hmpdacc.org)

51 assembled reference genomes from bacteria of genus *Escherichia, Citrobacter* or *Klebsiella*, isolated from healthy individuals for the Human Microbiome Project, were searched for the presence of colicin genes using blastp (9) on the predicted proteome (evalue < 0.01) and the same queries as above. 16 out of 51 (31%) were found to encode colicin-like

proteins aligning with our queries with more than 90% identity. The list of searched genomes and the results of the analysis can be found in Dataset S1.

BtuB homologs and phylogenetic tree

4,016 *Escherichia coli* proteomes from the NCBI database (05-12-2015) were searched for homologs of the BtuB sequence using *hmmsearch* (HMMER v. 3.1b2) (10) with a Hidden Markov Model (HMM) built out of the 20 most diverse sequences of NCBI conserved protein domain family PRK10641 (evalue < 10e-60). Only one representative was kept for sequences with more than 99% identity using usearch (v. 7.0) (11). A phylogenetic tree was built with the remaining sequences using *fasttree* with default parameters (12) (Fig. S24). The sequences belonging to each of the two clearly delimited branches were used to create an HMM for the core-genome BtuB and the divergent BtuB sequences. All *E. coli* genomes were searched again with both models using *hmmscan* (evalue < 10e-60) (10). When no BtuB homolog was found using this method, genomic sequences were checked with *tblastn* (9) (more than 90% coverage, presence of an initiation codon, no stop codon) to correct potential gene prediction mistakes. The list of searched genomes and the results of the analysis can be found in Dataset S3.

Construction of plasmids. Plasmids and oligonucleotides used in this study are listed in Tables S1 and S3, respectively. DNA manipulations were conducted using standard methods. Unless otherwise stated, KOD Hot Start DNA polymerase (Novagen) was used for all PCR reactions and all constructs were sequenced and confirmed to be correct before use. Oligonucleotides were synthesized by Sigma Genosys and restriction enzymes purchased from New England Biolabs.

To generate pGRG25-P*max*::*rfp*, the relevant fragment was amplified from pUltraRFP-GM, using oligonucleotides P1 and P2, digested with PvuI and NotI and ligated into PacI-NotI-digested pGRG25. To generate pGRG25-P*max*::*rfp-btuB*, the BZB1011 *btuB* gene controlled by its own promoter was amplified by PCR from BZB1011 genomic DNA using primers P3 and P4, and ligated into NotI-digested pGRG25-P*max*::*rfp*. To generate pGRG25-P*max*::*rfp-btuB*^{Alt}, the alternative *btuB* allele (*btuB*^{Alt}) was synthesized (Life Technologies) from the sequence of the *E. coli* 96.0497 genome (NCBI 417156405: c367415-365571) downstream of the BZB1011 *btuB* promoter region (320 bps upstream of the ATG), designed based on the genome of *E. coli* BZB1011 (W3110). The fragment was subsequently amplified by PCR using primers P3 and P5, and ligated into NotI-digested pGRG25-P*max*::*rfp*.

To generate pColA-Cm-Δ*lys*, pColE2-Cm-Δ*opn* and pColE2-Cm-Δ*tox*, pColA-Cm or pColE2-Cm were amplified by PCR using oligonucleotides P6/P7, P8/P9 and P10/P11, respectively (truncated whole-plasmid amplification using Phusion polymerase in HF buffer according to the New England Biolabs' protocol). Amplification products were purified, phosphorylated using T4 Polynucleotide Kinase (New England Biolabs) and self-ligated. The self-ligation region of the final plasmid was sequenced and found to be free of mutations.

Construction of bacterial strains. Bacterial strains used in this study are listed in Table S2.

GFP- or RFP-expressing strains were made using plasmids pGRG25-P*max*::*gfp* and pGRG25-P*max*::*rfp*, respectively. Briefly, the plasmids were transformed into the parental strain using electroporation. Recovery and incubation were carried out at 30°C. Resulting strains were grown overnight at 30°C in Lysogeny (LB) broth in the presence of 0.3% of L-arabinose. 5 µl of culture were streaked out on LB agar plates containing 0.3% L-arabinose

and cultured at 42°C overnight. Homogenously fluorescent isolated colonies were selected, streaked on LB agar plates and grown overnight at 42°C. Subsequently, homogenously fluorescent colonies were selected, streaked on LB agar plates and grown overnight at 37°C. Resulting strains were confirmed to be fluorescent, ampicillin-sensitive and toxic against the wild-type BZB1011 strain.

A colicin-resistant (*btuB* mutant) BZB1011 strain was produced by growing cells next to an E8 colicinogenic strain on 1.5% w/v LB agar medium. *De novo* resistant colonies were isolated, their *btuB* gene was amplified, and the amplification product was sequenced using primers P7-P9 (Table S3). In all cases, the *btuB* gene was found to be disrupted by an endogenous transposon. One of these strains was selected to be used as a colicin-resistant BZB1011 strain from this point onwards. Resistant colicin-A- and E2-producing strains were constructed by electroporating the pColA-Cm and pColE2-Cm plasmids, respectively, into the spontaneous *btuB* mutant of BZB1011 or in a fluorescently-labelled version of this strain generated as described above.

Complementation with the BZB1011 *btuB* receptor or the alternative *btuB* allele ($btuB^{Alt}$) was done by transforming the BZB1011 and BZB1011 (*btuB*) strains with pGRG25-P*max*::*rfp-btuB* and pGRG25-P*max*::*rfp-*$btuB^{Alt}$. In each case the transposon was mobilized and transferred to the chromosome, and the plasmid was subsequently eliminated as described above for the generation of GFP- or RFP-expressing strains.

Bacterial growth conditions. Unless otherwise indicated, all *E. coli* strains were grown overnight in 5 ml LB medium in 50 ml polypropylene tubes at 37°C with agitation (220 rpm). If needed, the medium was supplemented with chloramphenicol [34 μg ml^{-1}], kanamycin [50 μg ml^{-1}] or ampicillin [100μg ml^{-1}]. Competitions and mitomycin C experiments were carried out on 0.8% w/v LB agar medium, whilst 1.5% w/v LB agar medium was used for determination of colicin toxicity from spent culture supernatants and genetics. Unless otherwise indicated, LB agar plates were incubated statically at 37°C for 16 hours.

Colicin reporter assay. BZB1011 cells harboring the pUA66-P*colA*::*gfp* plasmid were grown to exponential phase. Wild-type BZB1011 and BZB1011 cells harboring pColA, pColE1, pColE2, and pColE4 were grown overnight and normalized for optical density at 600 nm (OD600) using the culture supernatant (spent media) from a BZB1011 overnight culture. Their supernatant was collected and filtered through a 0.22 μm Millipore filter. 2 μl of spent media from each strain were added to 198 μl of the exponential-phase bacteria harboring the reporter plasmid in a black microtitre plate with clear-bottomed wells, which was incubated in a Tecan Infinite 200 Pro multiwell plate reader at 37°C with agitation (220 rpm). OD600 and fluorescence (excitation: 395 nm, emission: 509 nm) were measured; OD600 was used to correct for variations in fluorescence readings due to differences in cell density.

Colicin E1 production assay. For the experiment shown in Fig. 1A normalized spent media from the wild-type BZB1011 strain and from BZB1011 cells harboring pColA, pColE2, and pColE4 were prepared as described for the colicin reporter assay. 1 ml of each spent medium was added to 4 ml of exponentially growing pColE1-containing BZB1011 cells and the resulting cell suspensions were split into two. The supernatants of the first set of suspensions were immediately collected by centrifugation. The cell pellets were resuspended into 300 μl Bugbuster Master Mix (Novagen) and added to the supernatants. The suspensions were subsequently filtered (0.22 μm). The second set of suspensions were incubated for 3 hours at 37°C with agitation (220 rpm) and then treated in the same way as above. Stationary-phase

bacteria from wild-type BZB1011 were diluted 1000-fold in LB medium, and 60 µl was spread on 1.5% w/v LB agar plates. 10 mm wells were made in the plates and filled with 130 µl of each supernatant. After 16 hours of incubation at 37°C, the zone of growth inhibition around the wells was measured at four points to compare the toxicities of the culture supernatants. For the experiment shown in Fig. S2B normalized spent media from the wild-type BZB1011 strain and from BZB1011 cells harboring pColA, pColE2-Cm, pColE2-Cm-Δ*opn*, pColE2-Cm-Δ*tox*, pColE7, and pColE8 were prepared as described for the colicin reporter assay. 1 ml of each spent medium or 1 ml of spent medium from the wild-type BZB1011 strain containing mitomycin C from *Streptomyces caespitosus* (Sigma-Aldrich) at a final concentration of 0.05 µg ml^{-1}, was added to 4 ml of exponentially growing pColE1-containing BZB1011 cells. Assessment of the effect of each spent medium on the toxin production level of the colicin E1-expressing cells was further performed using the same experimental setting as for Fig. 1A.

Growth rate measurements. Overnight liquid cultures were diluted into 200 µl of LB medium in 96-well microtitre plates at a starting OD600 of 0.001. Cells were grown with agitation (220 rpm) at 37 °C using a plate reader (Tecan, Infinite 200 Pro) and their OD600 was measured automatically every 900 s. Growth rates were calculated for individual wells as the slope of the linear regression of the natural logarithm of OD600 over time for OD600 > 0.1 and OD600 < 0.3.

Competition experiments. For all competition experiments, cells were harvested from overnight cultures, washed twice with LB medium, and resuspended and normalized in LB medium to an OD600 of 1.2. When required, cultures were further diluted in LB medium as indicated. Mixed communities were generated by combining the relevant strains in the appropriate ratios. 5 µl of bacterial suspensions were spotted onto 0.8% w/v LB agar plates, which were incubated statically at 37°C for 16 hours, unless otherwise indicated.

Mitomycin C assays and MIC determination. Cells were harvested from overnight cultures, washed twice with LB medium, and resuspended and normalized in LB medium to an OD600 of 1.2. Individual strains, or relevant mixtures were further diluted 1000-fold in LB medium. 5 µl of bacterial suspensions were spotted onto 0.8% w/v LB agar plates without or with added mitomycin C from *Streptomyces caespitosus* (Sigma-Aldrich) at a final concentration of 0.01 µg ml^{-1}. For determination of the mitomycin minimal inhibitory concentration (MIC) for the background strain BZB1011, the cell suspension of this strain was prepared in the same way as for the mitomycin C assays, and 5 µl of bacterial suspension were spotted onto 0.8% w/v LB agar plates containing mitomycin C at final concentrations starting from 0.2 µg ml^{-1} and reaching 2 µg ml^{-1}. Unless otherwise indicated, plates were incubated statically at 37°C for 16 hours.

Identification of the mutation in spontaneously-occurring btuB mutants. Spontaneous *btuB* mutants (presented in Fig. S23A) were generated by spotting 10 µl of a 1000-fold dilution of a BZB1011 P*max*::*gfp* overnight culture next to a 10 µl spot of undiluted overnight liquid culture of colicin-A-, E2- or E4-producing strains on 1.5% w/v LB agar medium. Fluorescent colonies growing at the interface between the two spots were carefully picked and re-isolated. The *btuB* sequence was PCR-amplified from colonies using primers P12-P14 (Table S3) and DNA sequenced (Sanger).

Test of the alternative btuB function. Normalized spent media from BZB1011 cells harboring pColE2 and pColE4 were prepared as described for the colicin reporter assay. The strains that

were tested (see Fig. S25) were grown to exponential phase (approximate OD600 of 0.4) and were further diluted in LB medium to OD600 of 0.07. The cell suspensions were spread onto the surface of 1.5% w/v LB agar plates using a sterile cotton swab. 10 mm wells were made in the plates and filled with 130 µl of each spent medium. After 16 hours of incubation at 37°C, the zone of growth inhibition around the wells was measured at four points to compare the toxicities of the culture supernatants.

Lysis assay. Spent medium of BZB1011 cells harboring pColE2 was prepared as described for the colicin reporter assay. 1 ml of spent medium was added to 4 ml of normalized exponentially growing (OD600 of 0.6) cultures of BZB1011 cells harboring pColA-Cm or pColA-Cm-Lys. Cell suspensions were incubated for 2 hours at 37°C with agitation (220 rpm). Serial dilutions of the resulting cell suspensions were subsequently platted on 1.5% w/v LB agar plates and incubated at 37°C for 16 hours.

Imaging and analysis. Imaging of bacterial spots was performed with a Leica M205FA fluorescent stereomicroscope (Leica Microsystems) using a 10x (NA 0.5) dry objective and the associated LAS X software. Images were processed using *FIJI/ImageJ* software (https://fiji.sc/). The same software was used for analysis of the area or fluorescence intensity of bacterial spots. For each experiment, the acquisition and processing of all microscopy images was done using identical settings throughout.

Statistical analyses. Statistical tests were performed with *R* (v 3.2.1) (http://www.R-project.org). For Fig. 1-3 relevant statistical analyses are given below.

Fig. 1. Panel A: Analysis of Variance (ANOVA) and multiple comparisons of means (MCM, Dunnett's test) confirmed that the increase in toxicity from time 0 to time 3h was significantly higher in extracts from cells exposed to E2 (DNase activity), compared to all other spent media ($p<0.001$). **Panel D:** ANOVA and MCM (Dunnett's test) confirmed that the area covered by the colicin-E2-producing strain, and no other, was significantly smaller than the area covered by the background strain against all toxin-producing strains except itself.

Fig. 2. Panel C: ANOVA and MCM (Dunnett's test) confirmed that the area of the mixed spot was significantly smaller compared to the reference (the same mixed spot vs the non-producer) when the competing colonies were E2 vs E1E4, and in no other case. **Panel E:** MCM (pairwise t-tests with Bonferroni correction) confirmed that the relative intensity of the resistant strain producing colicin E2 against mixed colicin-E1- and E4-producing competitors was significantly higher than for the non-producer and the colicin-A-producing strain (adjusted p-value<0.001).

Fig. 3. Panel C: MCM (pairwise t-tests with Bonferroni correction) confirmed that the overall fluorescence intensity was significantly lower when the colicin-E2 producer was mixed with two other producers (E1 and E4) than with the other competitor combinations (p-value<0.001). **Panel E:** The drop in fluorescence when the mixture of the two colicin producers was spotted on the mitomycin-C-containing plate compared to when it was spotted on plain LB agar medium was significantly larger than the drop in fluorescence of the individual colicin producers or the non-producer strain (pairwise t-tests with Bonferroni correction, p-value<0.001).

For SI appendix figures all relevant statistical tests are indicated in the figure legends.

SUPPLEMENTARY INFORMATION FIGURES

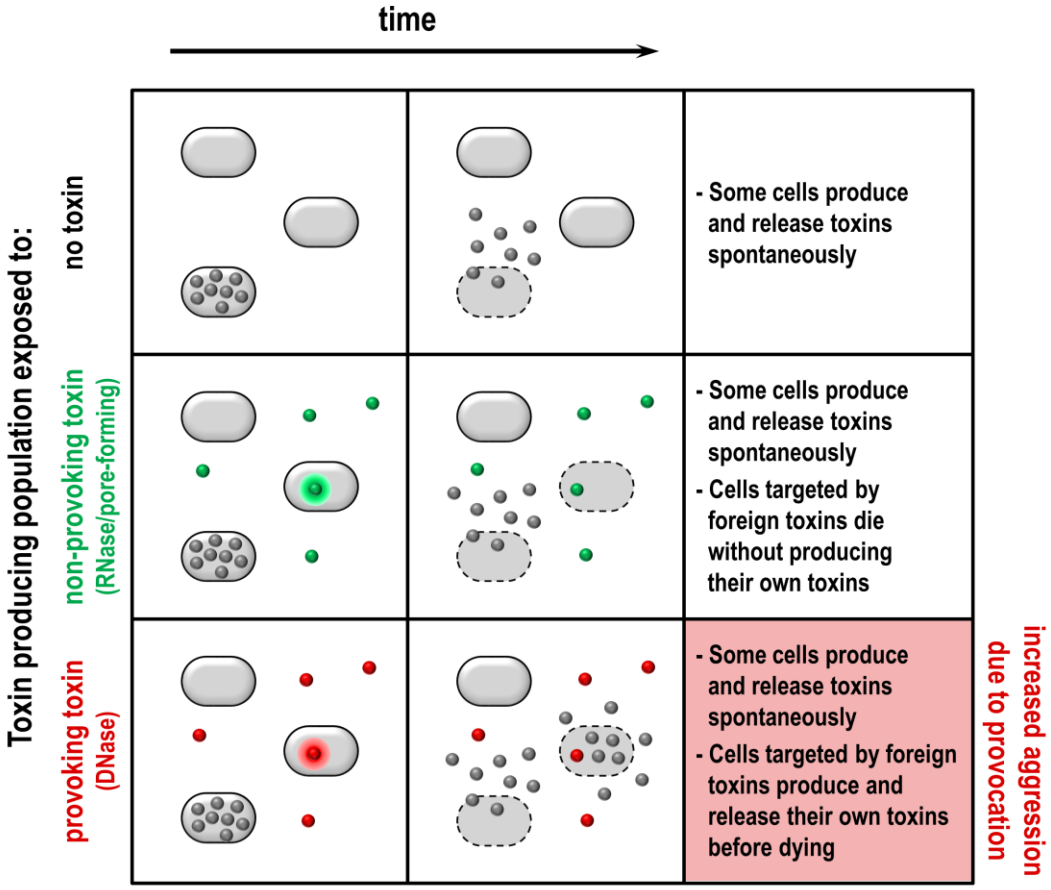

Fig. S1. Some bacterial toxins can function as aggression-provoking agents. In colicinogenic *Escherichia coli* populations, a small fraction of the cells spontaneously engages into toxin production and lyses, releasing massive amounts of toxins (grey spheres) (top row). Non-provoking (RNase- or pore-forming-) toxins produced by other strains (green spheres) are internalized by the focal population causing death without increasing the overall toxin release (middle row). Aggression-provoking (DNase-) toxins produced by other strains (red spheres) are internalized by the focal population, inducing toxin production prior to death by lysis, thereby increasing the aggression level (toxin production) of the focal population through provocation (bottom row).

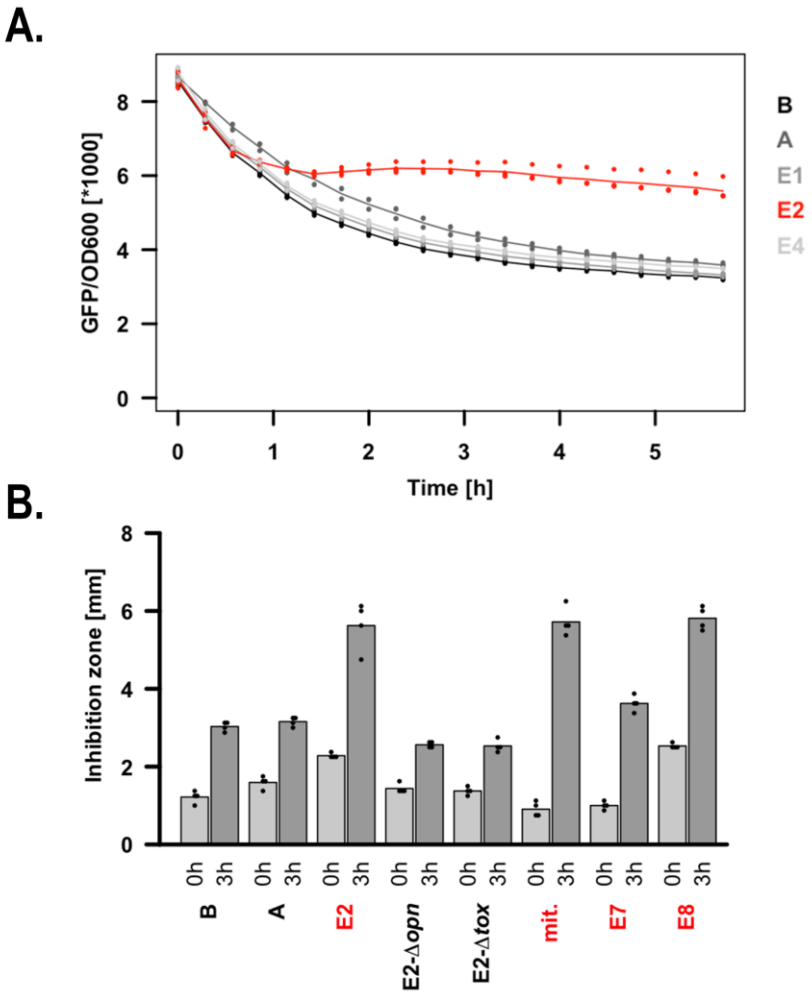

Fig. S2. Colicins with DNase activity increase the toxin production of other colicinogenic *E. coli* strains. A) *E. coli* strain BZB1011 reports increased toxin production when exposed to colicins with DNase, but not other, activities. Exponential culture of the background strain (BZB1011) harboring a reporter plasmid (pUA66-P*colA*) where the promoter of colicin A drives the transcription of GFP, was exposed to spent media from five strains (B: background non-colicinogenic sensitive strain; A and E1: pore-forming-colicin producers, E2 (in red): DNase-colicin producer; E4: RNase-colicin producer; see also Table 1). Fluorescence was measured during incubation at 37°C with agitation (220 rpm) and was normalized for growth. B) The ability to cause DNA damage via an active DNase toxin is essential for a colicinogenic strain to trigger retaliation. Cultures of a colicin-E1-producing strain were exposed to spent media from other *E. coli* strains for three hours. Spent media were extracted from cultures of BZB1011 (B), or BZB1011 encoding pColA (A), pColE2-Cm (E2, in red), pColE2-Δ*opn* (E2-Δ*opn*, the entire E2 operon is deleted from the plasmid), pColE2-Δ*tox* (E2-Δ*tox*, the E2 toxic domain is deleted from the colicin E2 coding sequence), pColE7 (E7, in red) and pColE8 (E8, in red); mitomycin C mixed into spent media from BZB1011 (mit., in red) was also added to a colicin-E1-producing culture at a final concentration of 0.01 µg/ml as a positive control for DNA damage. Extracts of the exposed cells were tested for toxicity using a growth inhibition assay. Analysis of Variance (ANOVA) and multiple comparisons of means (MCM, Dunnett's test) confirmed that the increase in toxicity from time 0 to time 3h was significantly higher in extracts from cells exposed to E2, E7, E8, and mit. (extracts capable of DNA damage), compared to all other spent media ($p<0.01$).

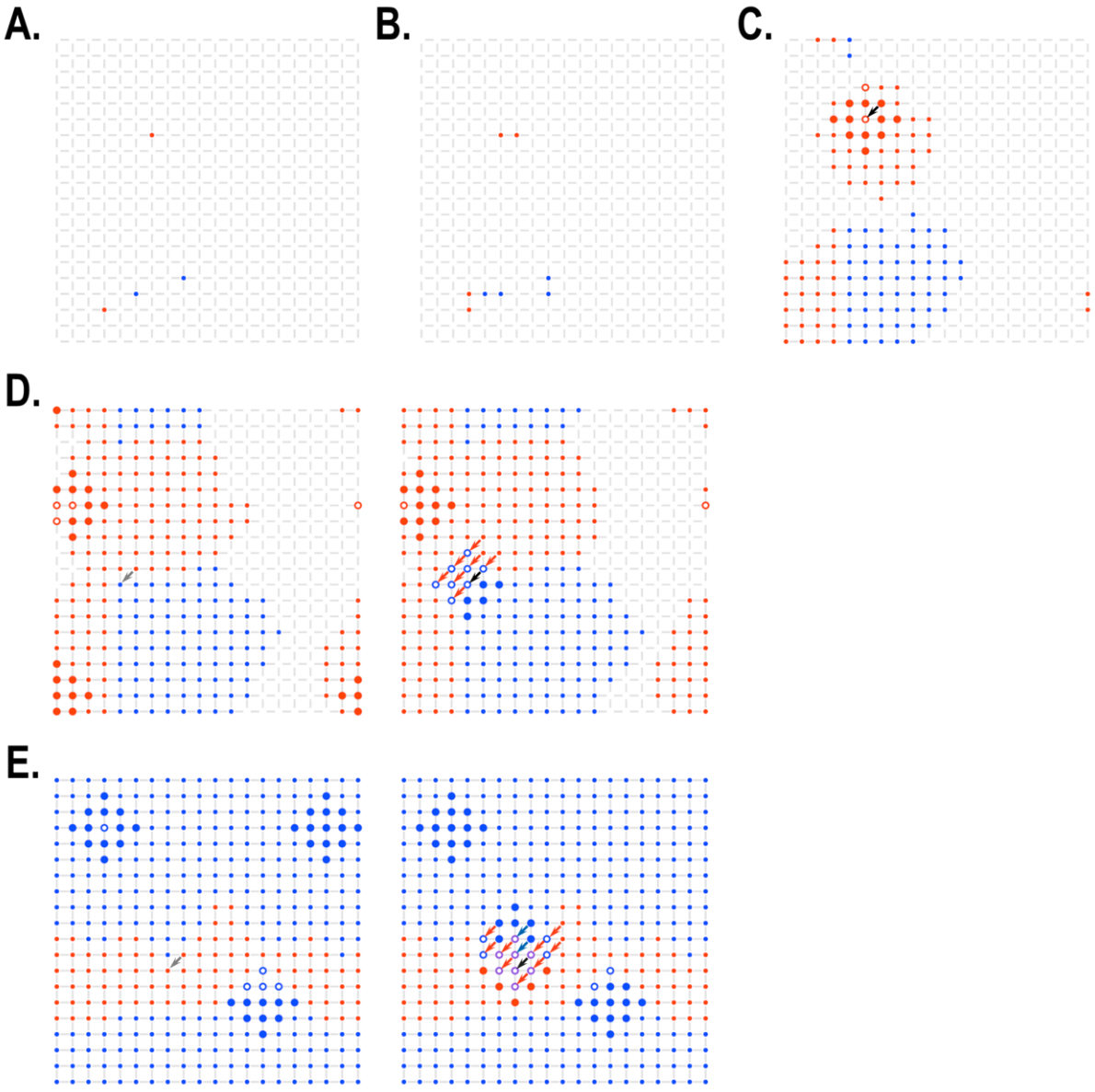

Fig. S3. Description of our lattice-based model for toxin-mediated competition in space. To confirm that the predictions of the ODE model also apply in space, we built a simplified lattice-based spatial model, which integrates cell growth, spontaneous and provocation-driven toxin production and toxin-driven cell death for two or three strains. Strains can produce no toxin, non-provoking toxins or provoking toxins. In addition, they can be sensitive or resistant to toxins produced by competing strains. The model uses lattices containing 20x20 vertices, each of which can be occupied by one cell at a time and by one or more toxins of different types simultaneously. Different colors represent different competing strains (small dot) and their corresponding toxins (same-color rings). When two toxins are present in the same vertex, a mixed color is used for the resulting toxin ring (for example toxins from a blue and a red strain will show in purple when they happen to be in the same vertex). A) A defined number of cells (unless indicated otherwise two for each strain) are randomly seeded in the beginning of each run. B) Cells produce one daughter cell per cycle which occupies one of the adjacent vertices at random, provided that these are not occupied by other cells (compare panels A and B). C) During every cycle, toxin-producing cells can spontaneously lyse and

release toxins which spread to the third order neighboring vertices and have a life-span of two cycles; spontaneous toxin production occurs with a probability of 0.005. In panel C, the position of a spontaneously-lysed producer (red strain) is indicated by a black arrow; after lysis, only its toxin (red ring) remains in that position. D) When a sensitive cell co-localizes in a vertex with a toxin produced by a competing strain, it dies. In panel D, a spontaneously-lysing cell (blue strain) is indicated by a grey arrow (left lattice) and its position after lysis is marked with a black arrow (right lattice). The positions of cells (red strain) dying because of foreign toxin (toxin from the spontaneously-lysed blue strain) are indicated by red arrows (right lattice). E) When the released toxin is a provoking one, sensitive colicinogenic cells die and release toxins with the same diffusion and life-span as spontaneously-lysing cells. In panel E, a spontaneously-lysing provoker (red strain) is indicated by a grey arrow (left lattice) and its position after lysis is marked with a black arrow (right lattice). Lysis of the red strain provokes two blue toxin producers which lyse and release their own toxin; their position after lysis is marked with blue arrows (right lattice). The positions of cells (from the blue or red strain) dying because of foreign toxins released spontaneously or due to provocation are indicated by red arrows (right lattice). For panels D and E, the lattices shown (left and right) were generated at the end of consecutive cycles of the same simulation run.

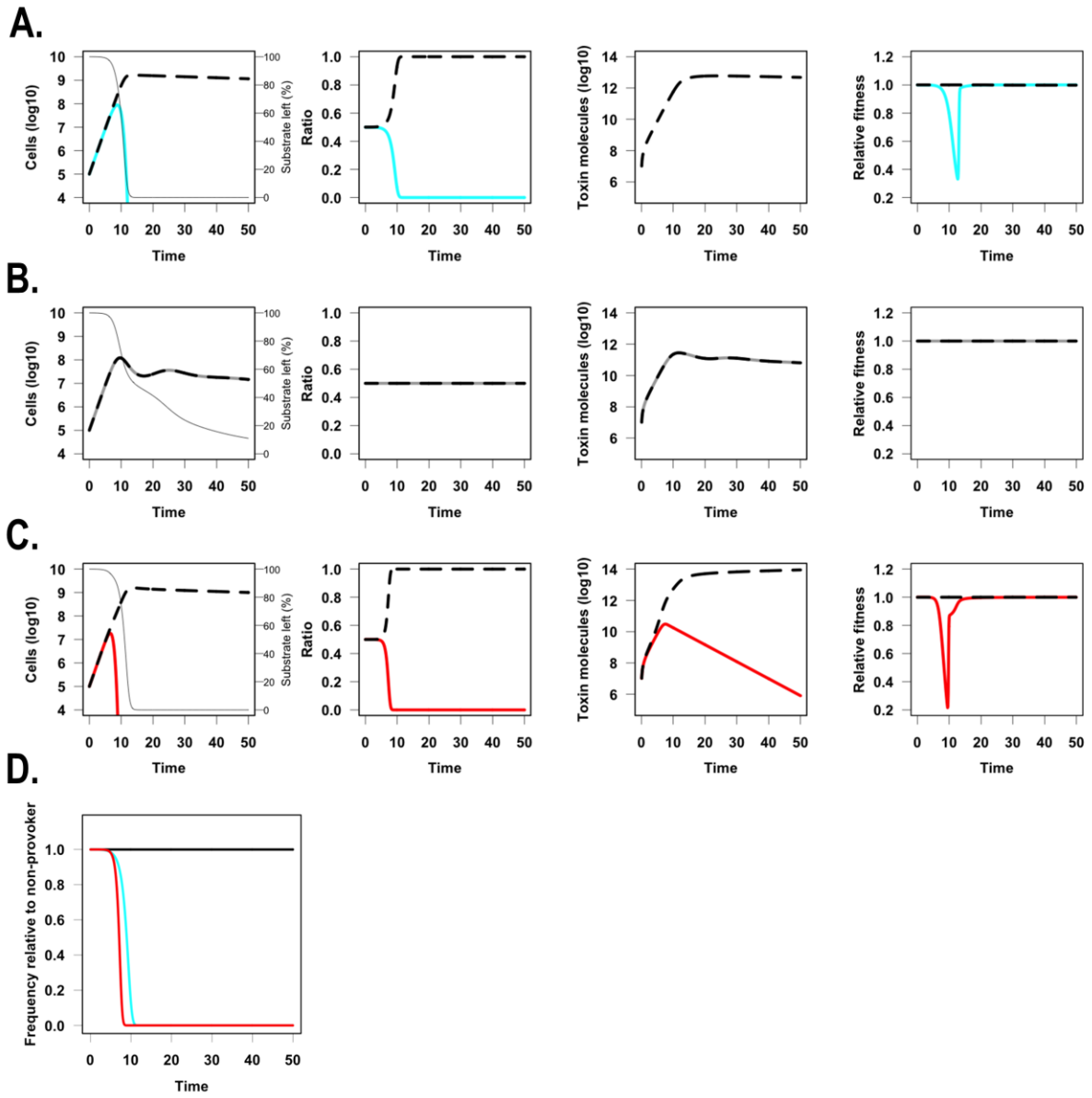

Fig. S4. Strains secreting aggression-provoking toxins are at a disadvantage in one-to-one competitions with other toxin-secreting strains. Graphs showing the dynamics of modeled populations (first column), the ratios between the strains (second column), the dynamics of the toxin population (third column), and the fitness (contribution of a strain to the whole population at the next time point) relative to the strain with the highest fitness (fourth column) as a function of time. The thin grey line in the first column represents the percent of substrate left relative to the beginning of the simulation. Encounters occur between pairs of strains of three possible types: a sensitive non-producer (cyan), a strain producing an aggression-provoking toxin (red) and a strain producing a non-provoking toxin (black or dark grey). The aggression-provoking strain decreases faster (C) than the sensitive strain (A) against a non-provoking-toxin producer; in competitions between non-provoking-toxin producers, synchronous fluctuations of the two populations tend to stabilize over time, when a balance between death, due to the competitor's toxin, and growth is reached (B). To make comparisons easier, panel D depicts the frequency of each focal strain relative to the non-provoking-toxin producer over time.

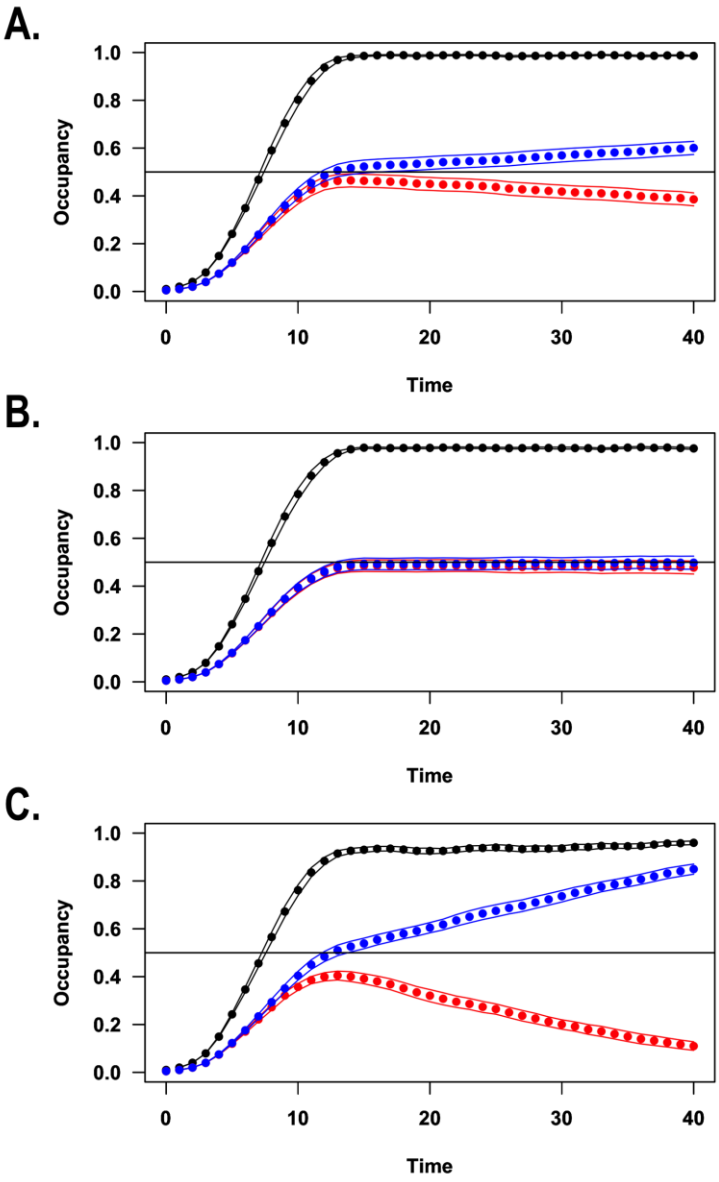

Fig. S5. In competitions between two cell types (blue and red) out of which at least one is a non-provoking-toxin producer, strains producing provoking toxins perform worse than either non-provoking-toxin producers or non-producers. Represented in red are the frequencies of the focal non-producer (A), the focal non-provoking-toxin producer (B) and the focal provoking-toxin producer (C). Represented in black is the occupancy of the lattice by all competing cell types (i.e. percentage of vertices occupied by any cell type). The figure summarizes the outcome of 40 simulation runs of 40 cycles using our lattice-based spatial model (described in Fig. S3). Dots represent the mean and fine lines the 97.5% confidence interval.

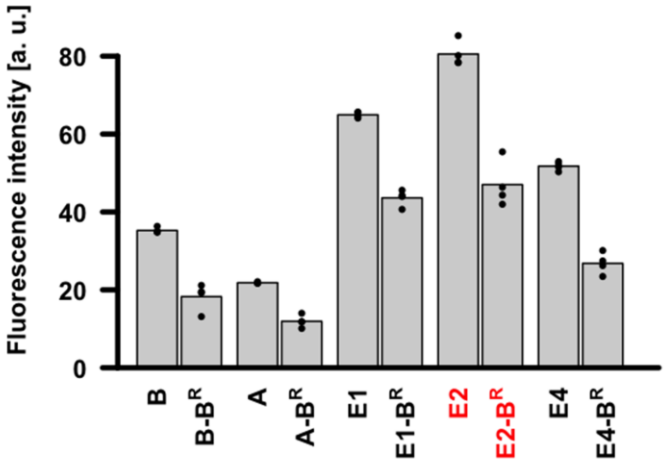

Fig. S6. Colonies growing next to each other compete for nutrients and space. GFP-labelled sensitive strains were spotted onto LB agar either on their own or next to a resistant non-producer (spotted at a 1000-fold higher density) and grown overnight. The GFP fluorescence of the sensitive strains was recorded. The difference is significant for all pairs (one-sided t-tests, p-value<0.01). B: background non-colicinogenic sensitive strain; A and E1: pore-forming-colicin producers, E2 (in red): DNase-colicin producer; E4: RNase-colicin producer; B^R: background non-colicinogenic resistant strain (see also Table 1).

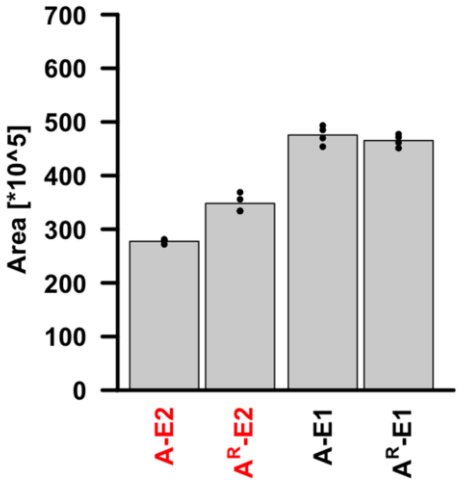

Fig. S7. An aggression-provoking-toxin producer (E2) performs better if its competitor is not sensitive to its toxin than if it is. Sensitive colicinogenic strains (aggression-provoking-toxin (E2-) producer, and non-provoking-toxin (E1-) producer) were spotted onto LB agar next to a sensitive or resistant pore-forming colicin producer (A or A^R, respectively) (spotted at a 1000-fold higher density) and grown overnight. The area occupied by the spot of the more dilute strain (E2 or E1) was recorded. The provoking-toxin producer (E2) elicits retaliation from the sensitive pore former (A) and performs worse than next to the resistant counterpart of this strain (A^R). The non-provoking-toxin producer (E1) performs the same next to the sensitive pore-forming toxin producer (A) as it does next to its resistant counterpart (A^R). The area of E2 colonies is significantly smaller when it is competing with A than with A^R (p-value<0.01, one-sided t-test), whereas no significant difference is found for E1. A and E1: pore-forming-colicin producers, E2 (in red): DNase-colicin producer; A^R resistant pore-forming-colicin producer (see also Table 1).

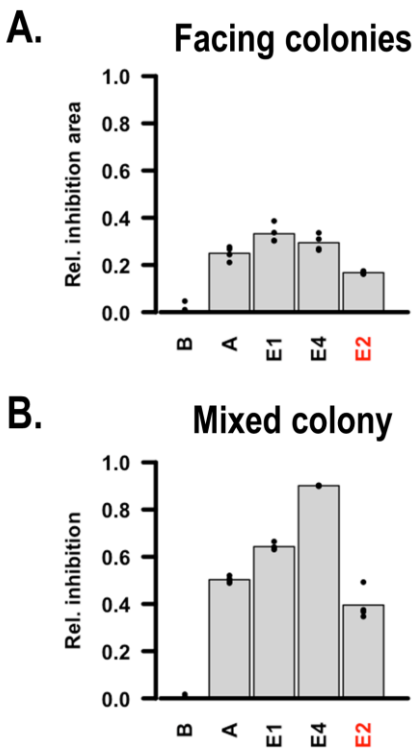

Fig. S8. The toxicities of each of the colicinogenic strains used in this study are comparable; the toxicity of the DNase-colicin producer tends to be lower than the toxicity of all other colicinogenic strains. A) 5 µl segregated spots of colicinogenic strains were placed next to a sensitive non-producing strain at different dilutions (1 vs 10^{-3}, respectively). Toxicity was determined by the area occupied by the spot of the more dilute sensitive non-producer. B) Mixed colonies containing a colicin producer and a sensitive strain in relevant ratios were generated. Toxicity was determined by quantifying by fluorescence intensity the residual amount of the sensitive strain in the mixed colony after overnight incubation. The toxicity of E2 is significantly lower than all other strains, except for B, both in facing colonies and in mixed colonies (p-value<0.05, pairwise one-sided t-tests with Bonferroni correction). For both panels, B: background non-colicinogenic sensitive strain; A and E1: pore-forming-colicin producers, E2 (in red): DNase-colicin producer; E4: RNase-colicin producer (see also Table 1).

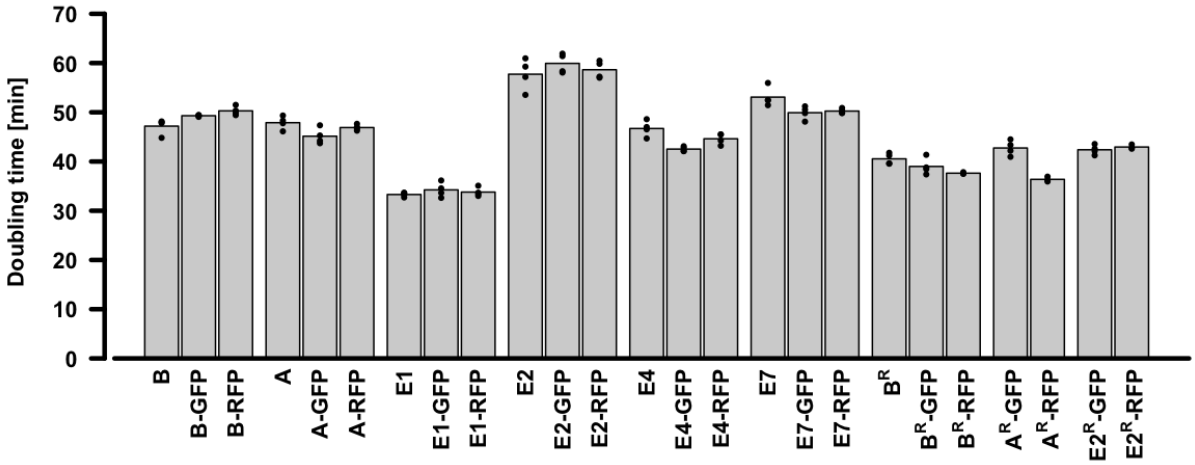

Fig. S9. Doubling times in exponential phase for all strains used in this study. Doubling times were calculated from growth curves done in LB medium; values between OD600 0.1 and 0.3 were taken into consideration for this calculation. For each strain the maximal doubling time of the unlabeled, GFP-labeled and RFP-labeled strain was determined. For strain annotation see Table 1.

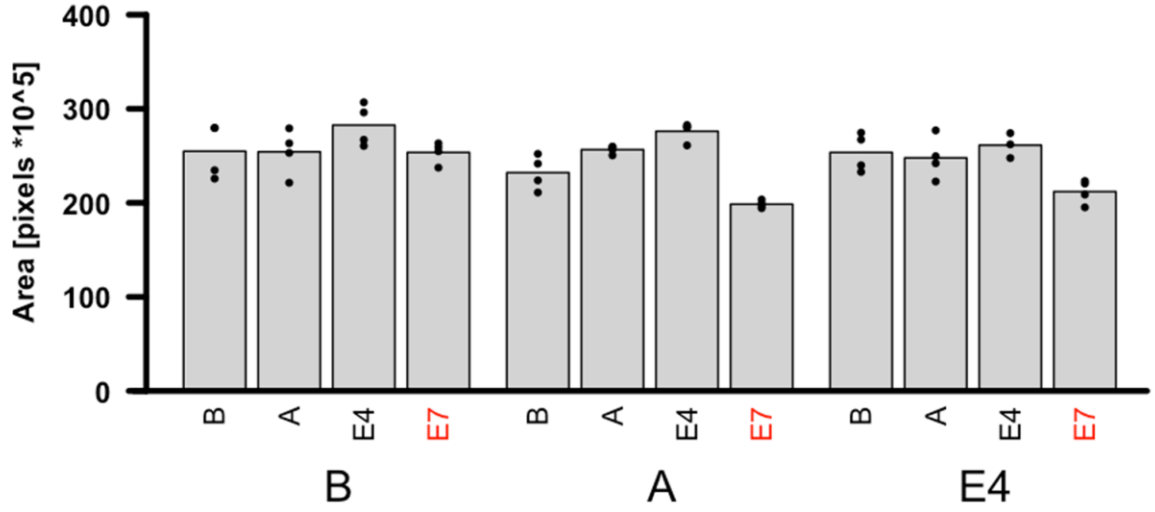

Fig. S10. *E. coli* strains producing colicins with DNase activity are at a disadvantage when competing one-to-one against other colicin-producing strains. Pairs of colicinogenic strains were spotted onto LB agar plates, each at a different dilution (1 vs 10^{-3}, respectively), and grown overnight. Large and small letters on the graph correspond to the concentrated and dilute spot, respectively. The area occupied by the spot of the more dilute strain was recorded. ANOVA and MCM (Dunnett's test) confirmed that the area covered by the colicin-E7-producing strain, and no other, was significantly smaller than the area covered by the reference strain against all toxin-producing strains. B: background non-colicinogenic sensitive strain; A: pore-forming-colicin producer, E7 (in red): DNase-colicin producer; E4: RNase-colicin producer (see also Table 1).

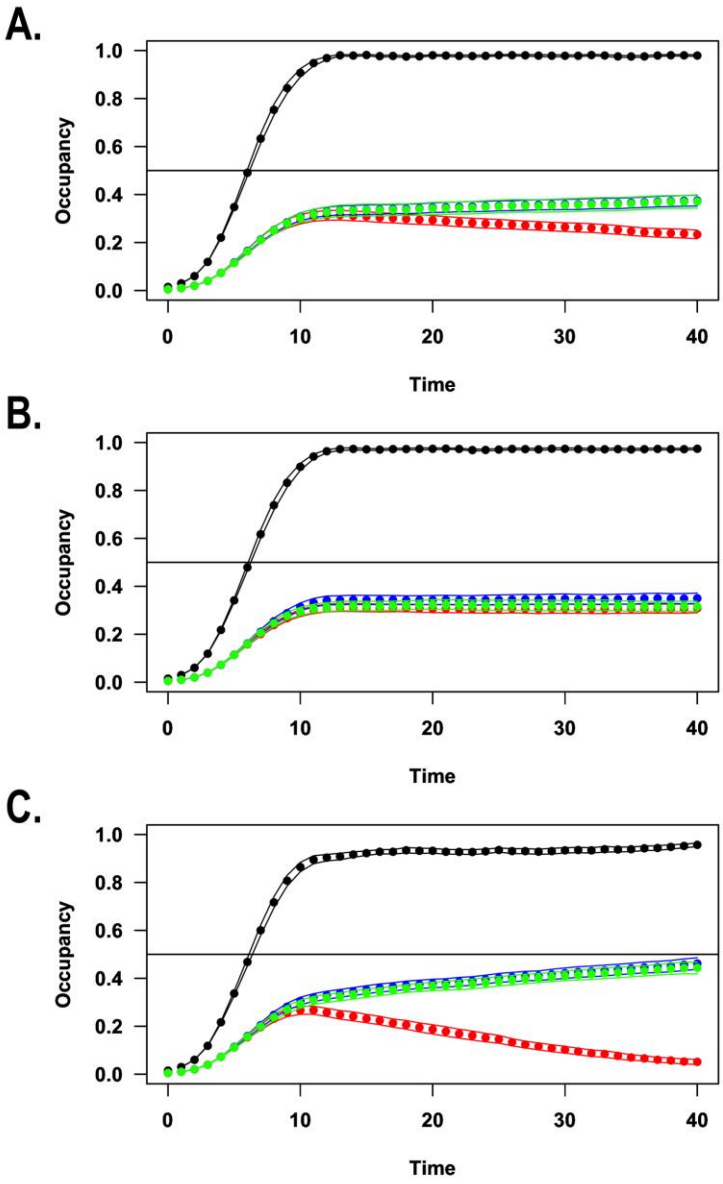

Fig. S11. In competitions involving three cell types (blue, green and red) out of which at least two are non-provoking-toxin producers, strains producing provoking toxins perform worse than either non-provoking-toxin producers or non-producers. Represented in red are the frequencies of the focal non-producer (A), the focal non-provoking-toxin producer (B) and the focal provoking-toxin producer (C). Represented in black is the occupancy of the lattice by all competing cell types (i.e. percentage of vertices occupied by any cell type). The figure summarizes the outcome of 40 simulation runs of 40 cycles of our lattice-based spatial model (described in Fig. S3). Dots represent the mean and fine lines the 97.5% confidence interval.

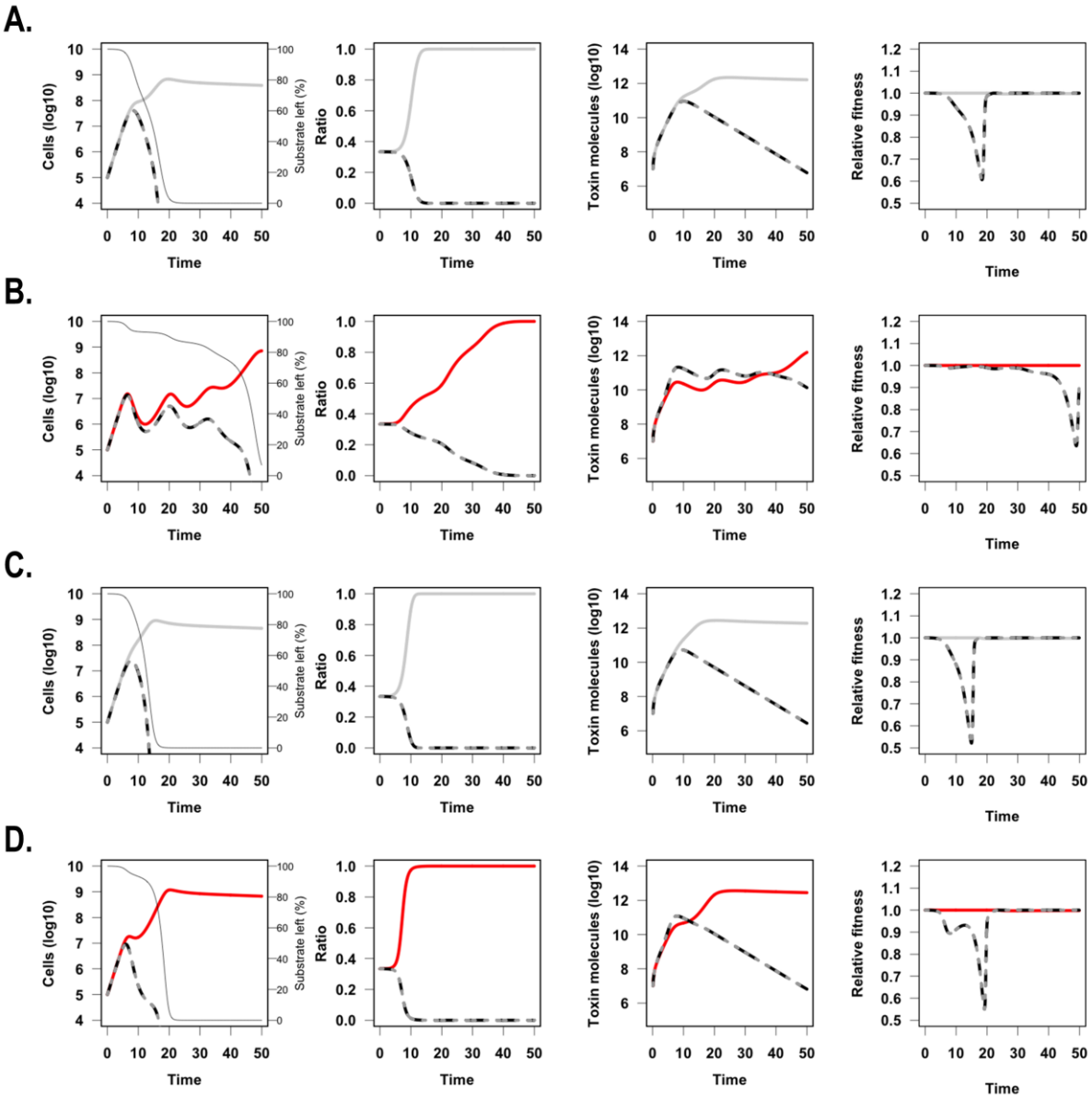

Fig. S12. When shielded from competitor's toxins, aggression-provoking strains quickly acquire an advantage compared to non-provoking strains in three-member communities. Graphs showing the competitions among three toxin-producing strains, including a focal strain segregated from its competitors. Segregation implies that the probability of the focal strain to reach or be reached by its competitors is lower by a factor *u* (segregation factor) compared to the probability of its two competitors to reach each other. A) and B) show the results for $u = 2$; C) and D) show the results for $u = 4$. A) and C) show the dynamics when the segregated strain is a non-provoking strain (light grey); B) and D) show the same for an aggression-provoking strain (red). For each simulation, the graphs show the dynamics of modeled populations (first column), the ratios between the strains (second column), the dynamics of the toxin population (third column) and the fitness relative to the strain with highest fitness (fourth column) as a function of time. The thin grey line in the first column represents the percent of substrate left relative to the beginning of the simulation. The model predicts that the stronger the segregation is, the more an aggression-provoking strain would benefit compared to a non-provoking strain.

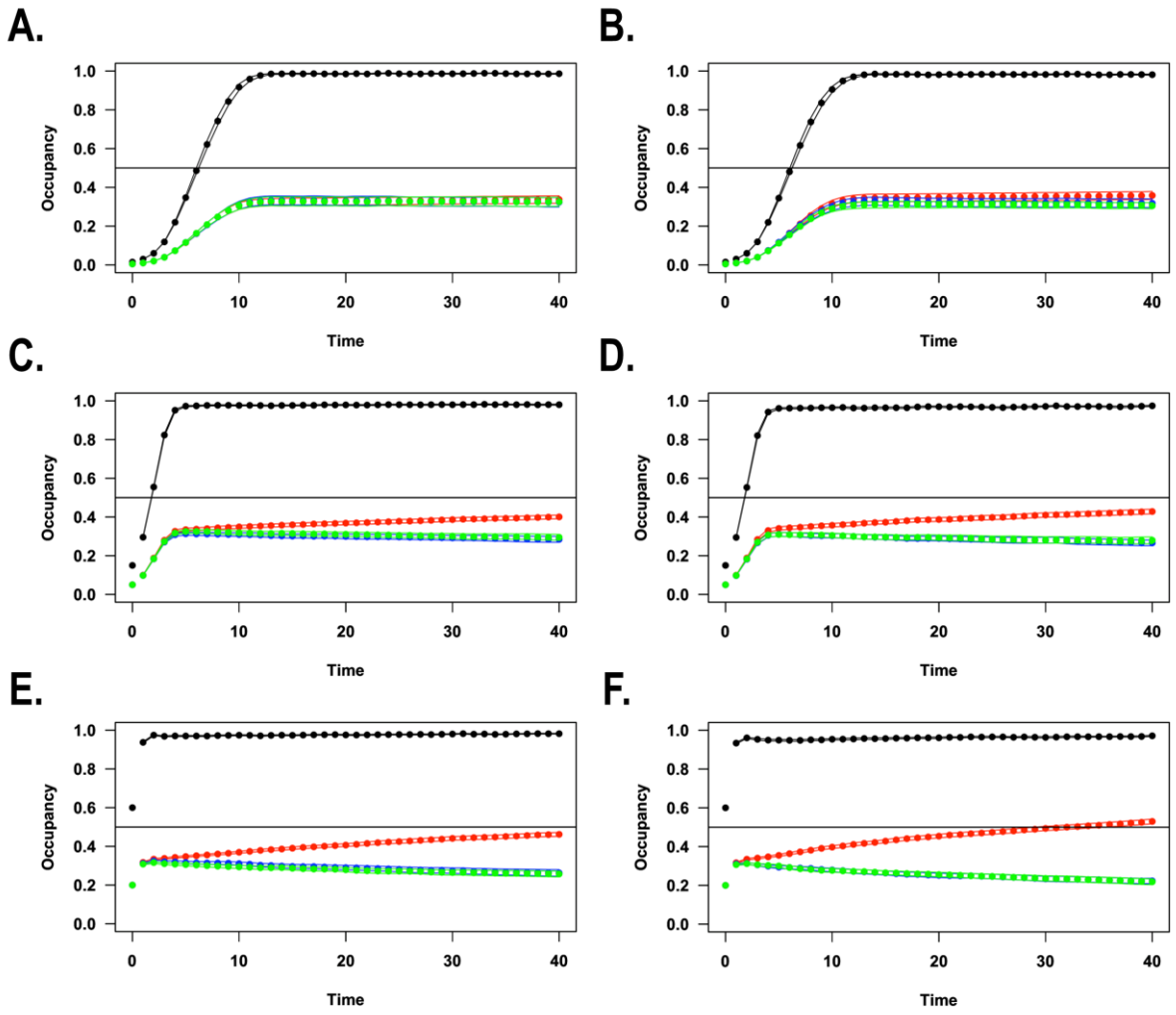

Fig. S13. In competitions against two non-provoking-toxin producers, a provoking-toxin producer performs better than a non-provoking-toxin producer if there is toxin-exposure asymmetry between the focal strain and its competitors (competition between blue, green and red cell types). In these simulations, the efficiency of the toxins has been modified so that the probability of the focal strain to kill, or to be killed by, its competitors is five times lower than the probability for the two competitors to kill each other. Represented in red are the focal non-provoking-toxin producer in panels A, C, and E and the focal provoking-toxin producer in panels B, D and F. Represented in black is the occupancy of the lattice by all competing cell types (i.e. percentage of vertices occupied by any cell type). The figure summarizes the outcome of 40 simulation runs of 40 cycles of our lattice-based spatial model (described in Fig. S3). As the spatial heterogeneity increases, the provoking strain has an increasing advantage (compare pairs AB, CD and EF). When simulations are started using two random seeds for each strain, this leads to the formation of large patches of clonal cells (panels A and B), whereas when twenty (C and D) or eighty (E and F) random seeds are used, smaller clonal patches are generated. The latter benefits the provoker more than the non-provoker. Dots represent the mean and fine lines the 97.5% confidence interval.

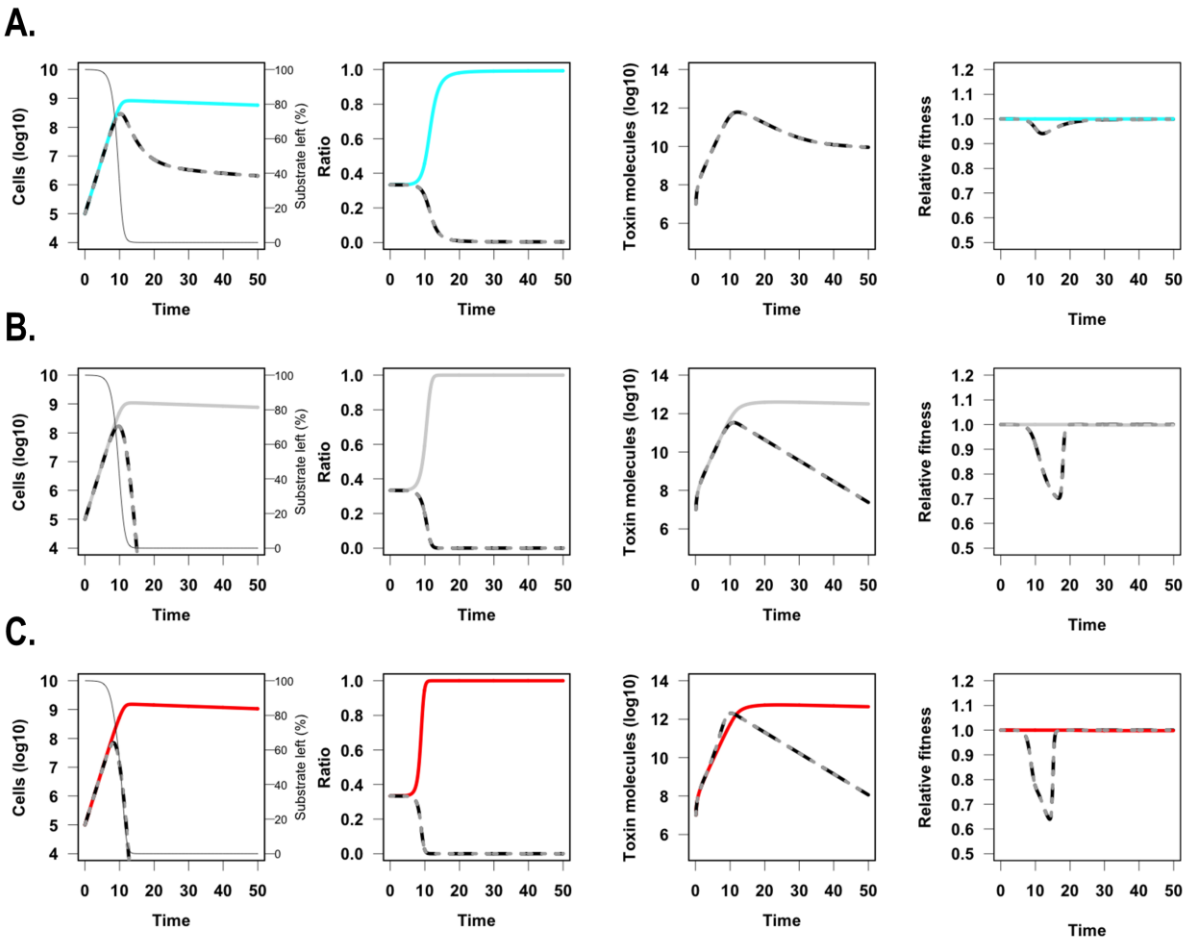

Fig. S14. When resistant to competitor's toxins, aggression-provoking strains benefit in three-member communities. Graphs showing the dynamics of modeled populations (first column), the ratios between the strains (second column), the dynamics of the toxin population (third column) and the fitness relative to the strain with highest fitness (fourth column) as a function of time in simulations where two non-provoking-toxin producers compete with a resistant non-producer (cyan) (A) or a toxin producer which can be either a non-provoker (light grey) (B) or an aggression-provoking strain (red) (C). The thin grey line in the first column represents the percent of substrate left relative to the beginning of the simulation. In this model, the aggression-provoking strain (red) defeats its toxin-producing competitors (in black or dark grey) faster than a non-provoking strain (light grey) or a resistant non-producer (cyan).

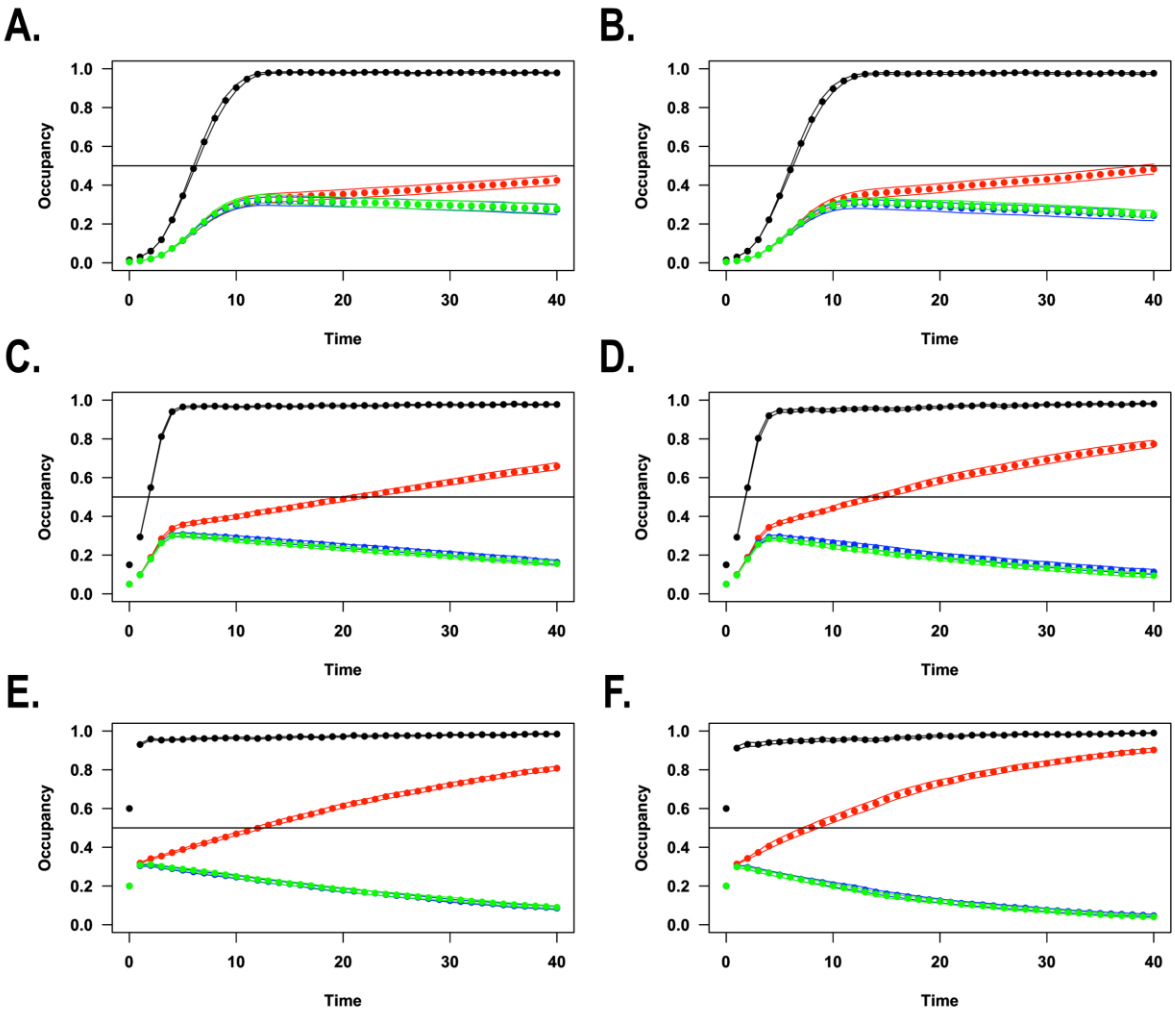

Fig. S15. In competitions against two non-provoking-toxin producers, a resistant provoking-toxin producer has a strong advantage compared to a resistant non-provoking-toxin producer (competition between blue, green and red cell types). Represented in red are the focal resistant non-provoking-toxin producer in panels A, C, and E and the focal resistant provoking-toxin producer in panels B, D and F. Represented in black is the occupancy of the lattice by all competing cell types (i.e. percentage of vertices occupied by any cell type). The figure summarizes the outcome of 40 simulation runs of 40 cycles using our lattice-based spatial model (described in Fig. S3). As the spatial heterogeneity increases, the provoking strain has an increasing advantage (compare pairs AB, CD and EF). When simulations are started using two random seeds for each strain, this leads to the formation of large patches of clonal cells (panels A and B), whereas if twenty (C and D) or eighty (E and F) random seeds are used, smaller clonal patches are generated. The latter benefits the resistant provoker more than the resistant non-provoker. Dots represent the mean and fine lines the 97.5% confidence interval.

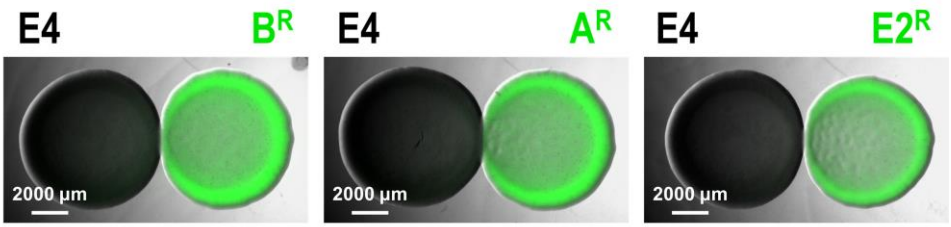

Fig. S16. Resistant DNase-colicin producers have no advantage over other resistant strains in one-to-one competitions with sensitive colicin producers. Sensitive colicinogenic strains were spotted onto LB agar plates next to GFP-labelled strains resistant to colicins, at different dilutions (1 vs 10^{-3}, respectively), and grown overnight. All resistant strains were found to be equally unaffected by the colicin producer growing next to them. A representative set of all pairs containing the sensitive colicin-E4 producer is shown. E4: RNase-colicin producer. B^R: background non-colicinogenic resistant strain; A^R: resistant pore-forming-colicin producer, $E2^R$: resistant DNase-colicin producer (see also Table 1).

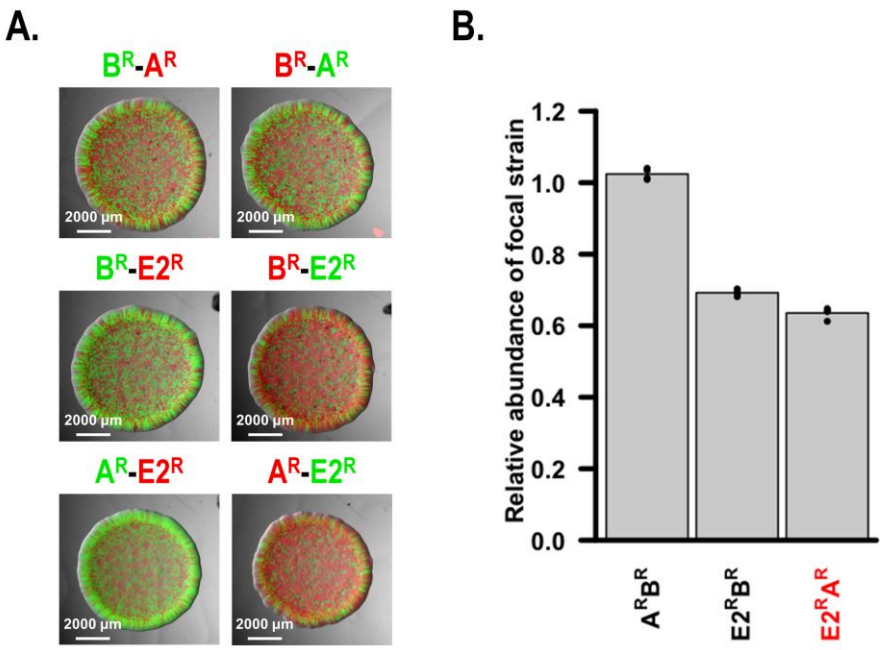

Fig. S17. Outcome of pairwise competitions between the three resistant strains used in this study. A) A mixture of two resistant strains, one labeled with GFP and the other labelled with RFP, was spotted onto LB agar and grown overnight. B) The fluorescence intensity of each strain was measured. The graph shows the ratios between the abundance of the two strains. B^R: background non-colicinogenic resistant strain; A^R: resistant pore-forming-colicin producer, $E2^R$: resistant DNase-colicin producer (see also Table 1)

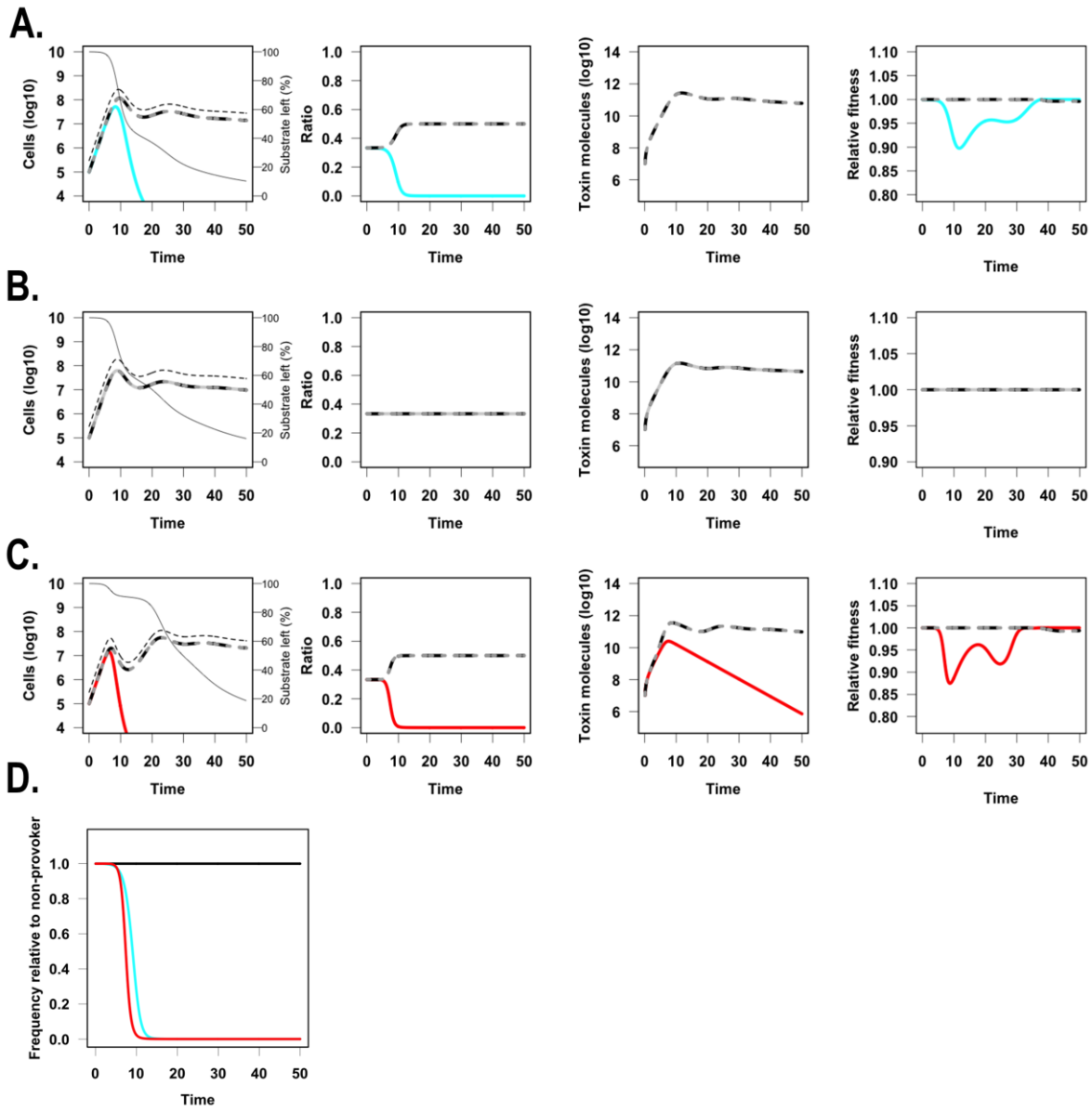

Fig. S18. The productivity of three-member communities is hampered when an aggression-provoking strain is present. Graphs showing the dynamics of modeled populations (first column; including the summed population of all three strains shown by the dotted thin grey line), the ratios between the strains (second column), the dynamics of the toxin population (third column) and the fitness relative to the strain with highest fitness (fourth column) as a function of time in simulations where two non-provoking-toxin producers compete against a sensitive strain (A, sensitive in cyan), a third non-provoking-toxin producer (B) or an aggression-provoking-toxin producer (C, aggression-provoking strain in red). The solid thin grey line in the first column represents the percent of substrate left relative to the beginning of the simulation. When and while an aggression-provoking strain is frequent in the community, the overall productivity is heavily impacted (C). To make comparisons easier, panel D gives the frequency of each focal strain relative to the non-provoker toxin producer over time.

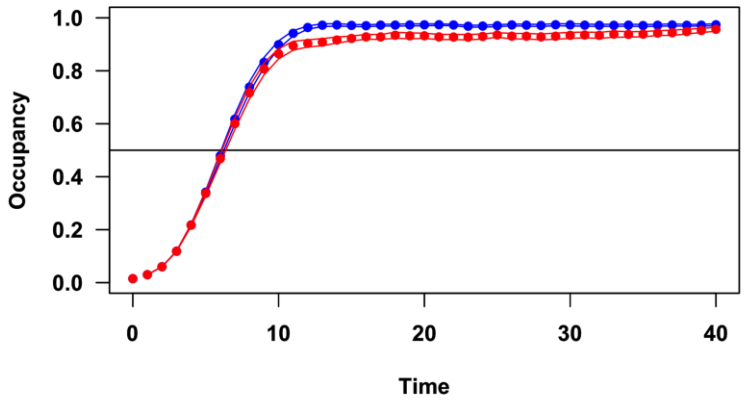

Fig. S19. The presence of a provoking-toxin producer in a three-member community decreases its productivity compared to a non-provoking-toxin producer. The overall productivity of the bacterial community is plotted in blue and red when a non-provoking-toxin producer and a provoking-toxin producer are included, respectively. The figure summarizes the outcome of 40 simulation runs of 40 cycles of our lattice-based spatial model (described in Fig. S3). Dots represent the mean occupancy of the lattice when all strains are considered, and fine lines represent the 97.5% confidence interval.

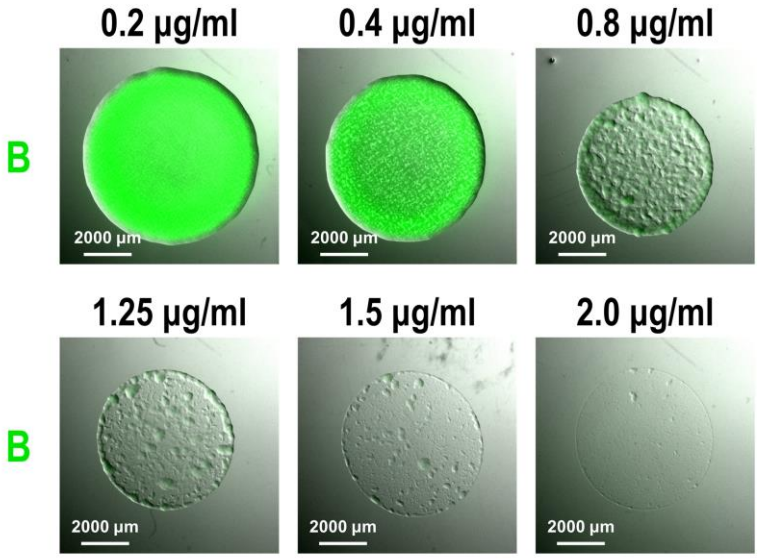

Fig. S20. The minimal inhibitory concentration (MIC) of Mitomycin C for the background strain in the experimental settings used in this study is 2 µg ml^{-1}. A 1000-fold dilution of a GFP-labelled BZB1011 (labelled B) overnight culture at OD600 1.2 was spotted onto LB agar containing increasing concentrations of mitomycin C. The MIC is the lowest concentration of the chemical where no growth was observed (bottom right panel).

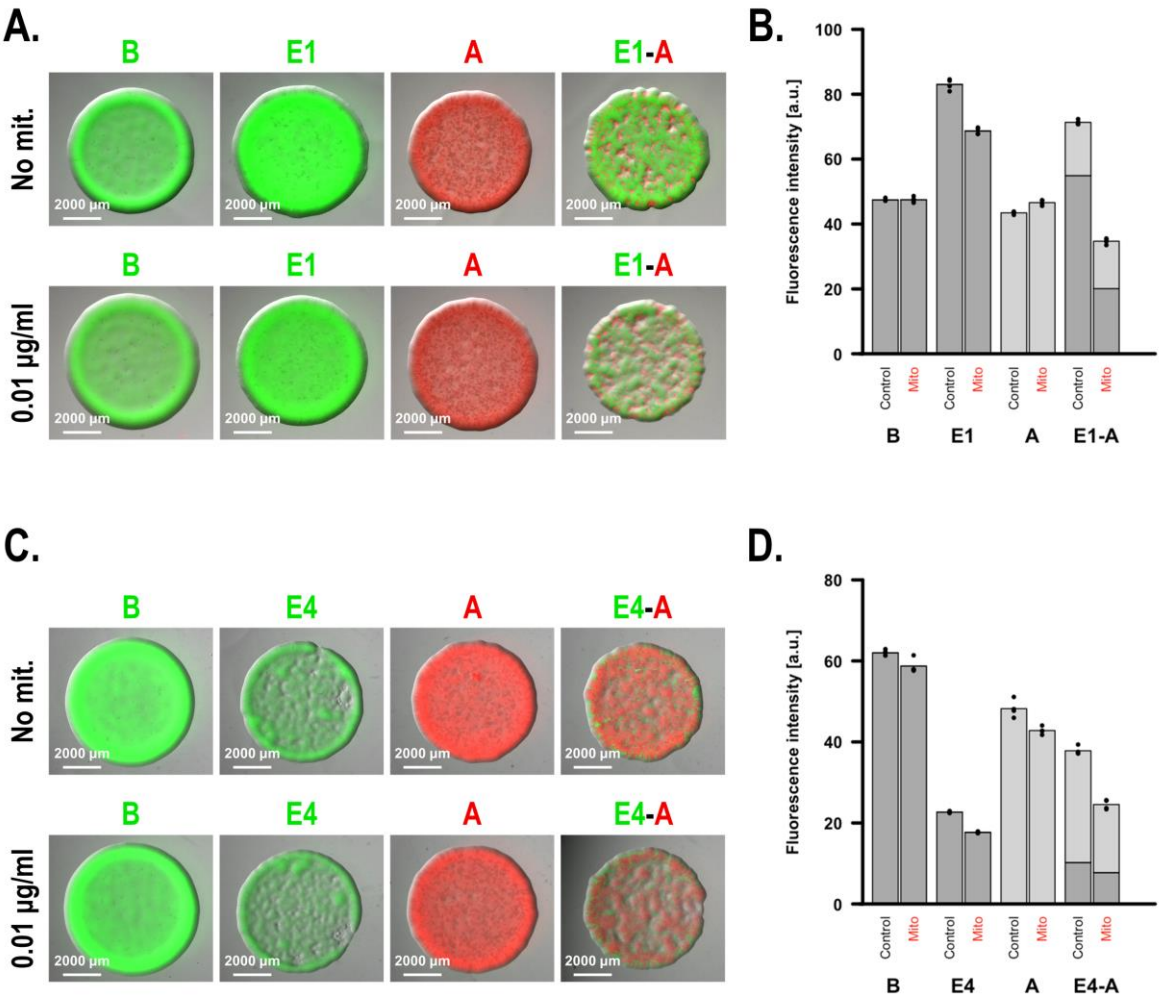

Fig. S21. Like toxins with DNase activity, DNA damaging chemicals reduce the productivity and disrupt the strain balance in toxin-secreting colicinogenic communities. A) and B) A 1000-fold dilution of overnight cultures of colicin-E1- and colicin-A-producing strains (GFP- and RFP-labeled, respectively) at OD600 1.2 were mixed at a ratio of 1 to 9 and spotted, together with controls, onto LB agar with or without added mitomycin C at a final concentration of 0.01 µg ml^{-1}. After incubation for 8 hours, the intensity of the fluorescence was measured (A). The summed RFP and GFP fluorescence values are plotted (B). C) and D) The same as in (A) and (B) was performed except that equal amounts of colicin-E4- and colicin-A-producing strains (GFP- and RFP-labeled, respectively) were used. The drop in fluorescence when the mixture of the two colicin producers was spotted on the mitomycin-C-containing plate compared to when it was spotted on plain LB agar medium was significantly larger than the drop in fluorescence of the individual colicin producers or the non-producer strain (pairwise t-tests with Bonferroni correction, p-value<0.001). For all panels, B: background non-colicinogenic sensitive strain; A and E1: pore-forming-colicin producers, E2: DNase-colicin producer; E4: RNase-colicin producer (see also Table 1).

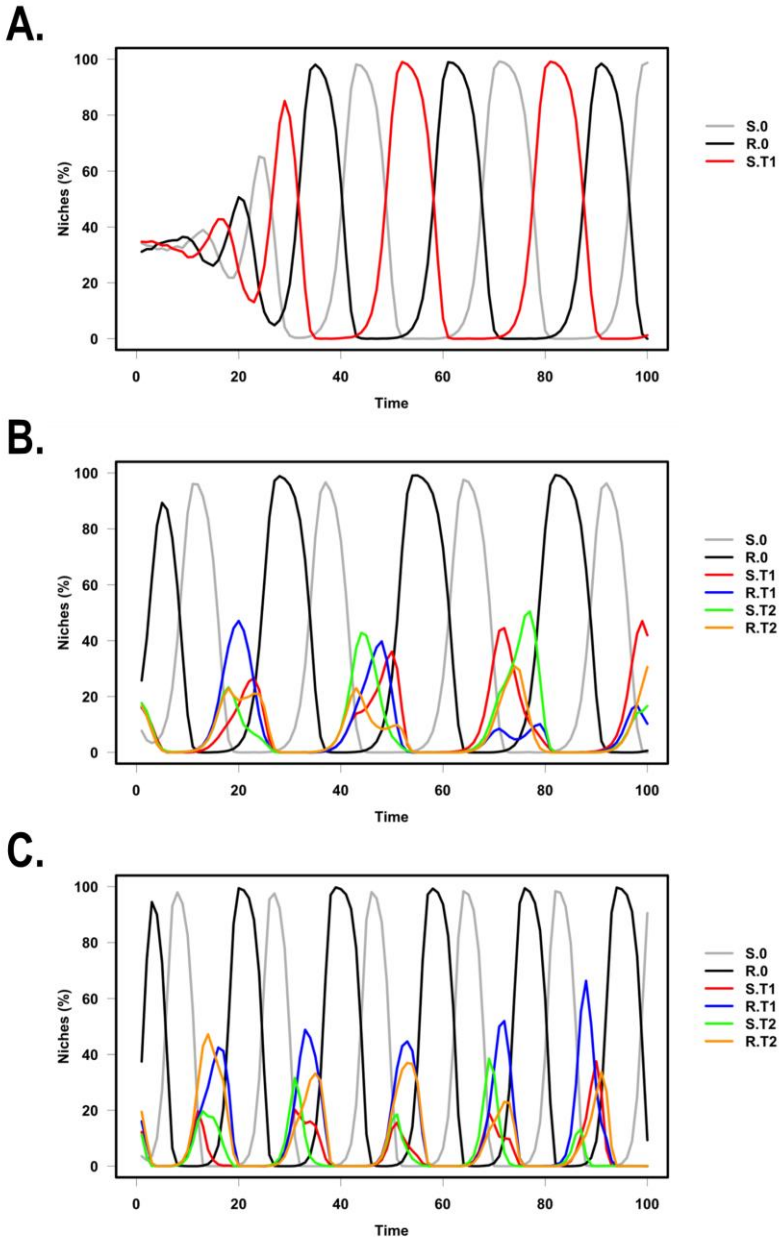

Fig. 22. In meta-communities comprising sensitive and resistant toxin-producing strains and sensitive and resistant non-producers, strain dominance varies periodically over time and multiple sensitive and resistant toxin-producers can co-exist during specific phases. The graphs show the population dynamics of strains which compete for a fixed number of niches. At each round, two (or three) strains, randomly selected from the strains dominating in the previous round, compete with one another; a small proportion of the initial strain set is kept in the game at all times to avoid extinctions, simulating a constant low migration rate. The main strain types are:1) toxin producers sensitive to other toxins; 2) toxin producers resistant to other toxins; 3) resistant non-producers; 4) sensitive non-producers. The outcome of the competition is decided based on a rock-paper-scissor model where several intuitive rules apply: i) toxin-producers outcompete sensitive non-producers; ii) toxin-production has a higher cost than resistance; iii) resistance has a higher cost than non-production; iv) the costs of toxin production and resistance cumulate. This is a simplified model, mainly intended for illustration. For spatial or more realistic models, see (7, 8). A)

Results for a system comprising three strains (sensitive non-producer [S.0], resistant non-producer [R.0], sensitive toxin producer [S.T1]), competing in pairs. B) Results for a system comprising six strains (sensitive non-producer [S.0], resistant non-producer [R.0], sensitive toxin-T1 producer [S.T1], resistant toxin-T1 producer [R.T1], sensitive toxin-T2 producer [S.T2], resistant toxin-T2 producer [R.T2]), competing in pairs. C) Results for a system comprising six strains (as in B), competing in sets of three strains.

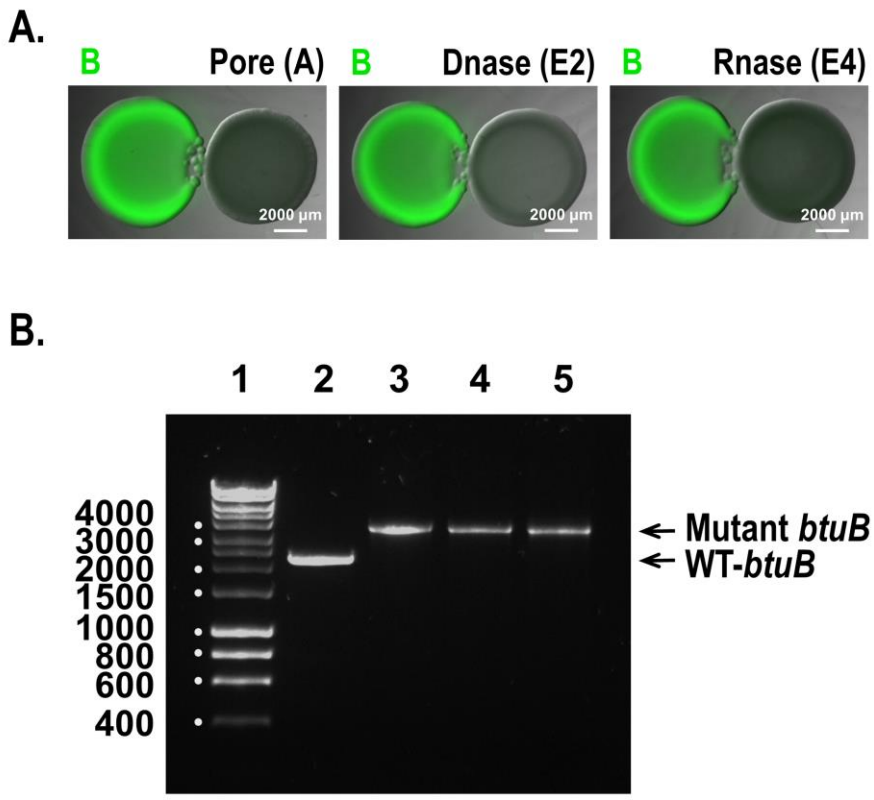

Fig. S23. Resistance to colicins arises readily in both colicinogenic and non-colicinogenic strains in experimental settings and is due to endogenous transposon insertions interrupting the *btuB* receptor gene. A) Colicinogenic strains were spotted onto LB agar plates next to a GFP-labelled sensitive non-producer at different dilutions (1 vs 10^{-3}, respectively) and grown overnight. GFP-fluorescent resistant colonies grow in the zone of inhibition of the sensitive strain. B) Resistance to colicins arises due to endogenous transposon insertions interrupting the *btuB* receptor gene. A resistant colony from each competition in (A) was re-isolated and the *btuB* gene of the cells was amplified by PCR; the *btuB* gene of the wild-type strain was also amplified as a control. The PCR products were subjected to electrophoresis on a 1% w/v agarose gel. Lane 1 contains DNA standards (Hyperladder I, Bioline), lane 2 the amplified *btuB* product of the wild-type strain and lanes 3-5 the amplified *btuB* products from cells becoming resistant after exposure to colicin A, E2 and E4, respectively. The size of the *btuB* gene amplified from the resistant cells is noticeably larger than that of the wild-type strain. All amplified *btuB* products from the resistant strains were sequenced, and all three were interrupted by the endogenous IS2 element from the BZB1011 strain.

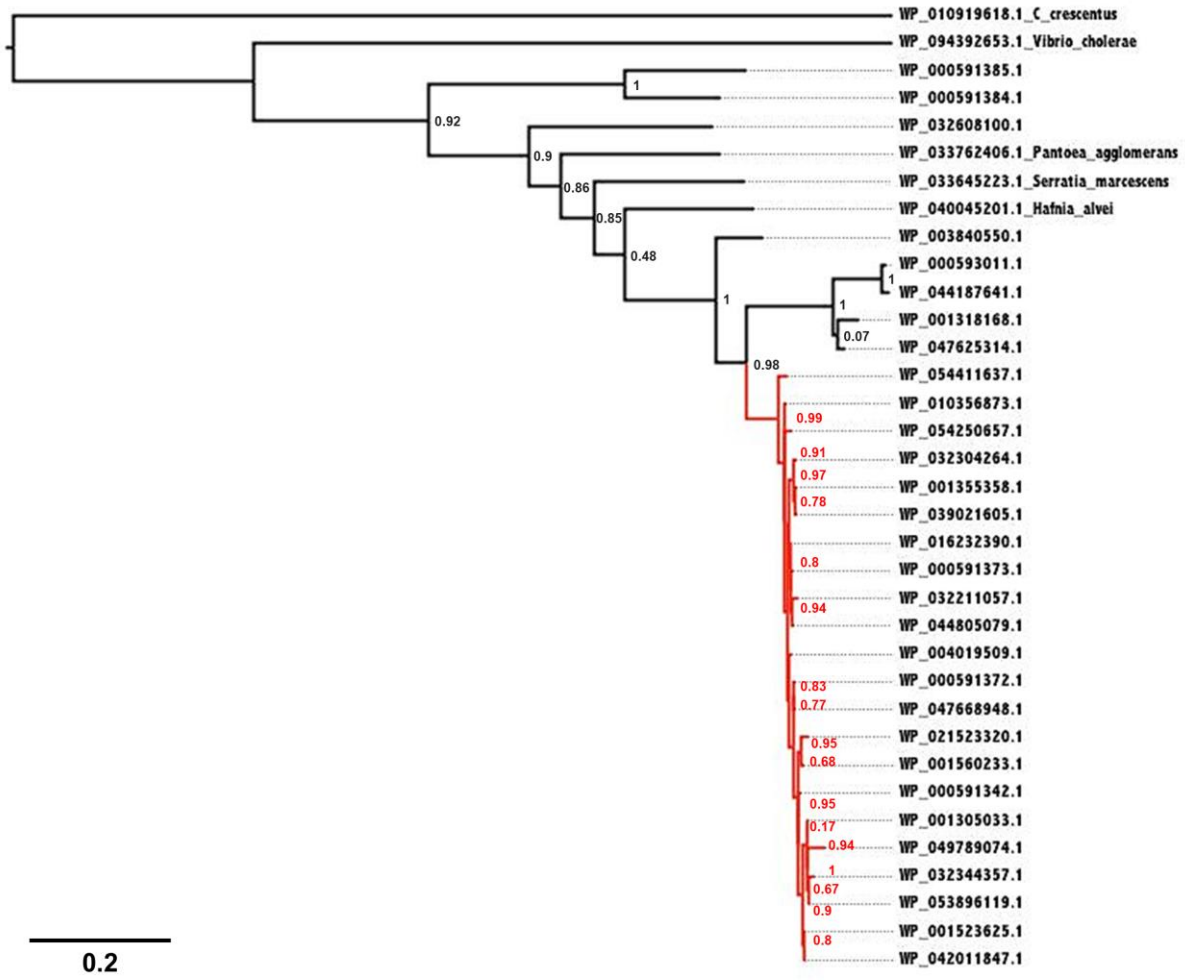

Fig. S24. *E. coli* genomes often (~ 7%) encode a divergent BtuB variant besides the core BtuB receptor protein. The protein sequences of BtuB homologs were retrieved from 4,016 *E. coli* genomes; one sequence was kept from each of the clusters predicted by ucluster (identity more than 99%). Sequences were aligned with muscle (13) and a phylogenetic tree was built with fasttree (12). The BtuB sequences belonging to the core genome of *E. coli* are shown in red; the divergent sequences (shown in black together with reference sequences) have a variable origin within Enterobacteria.

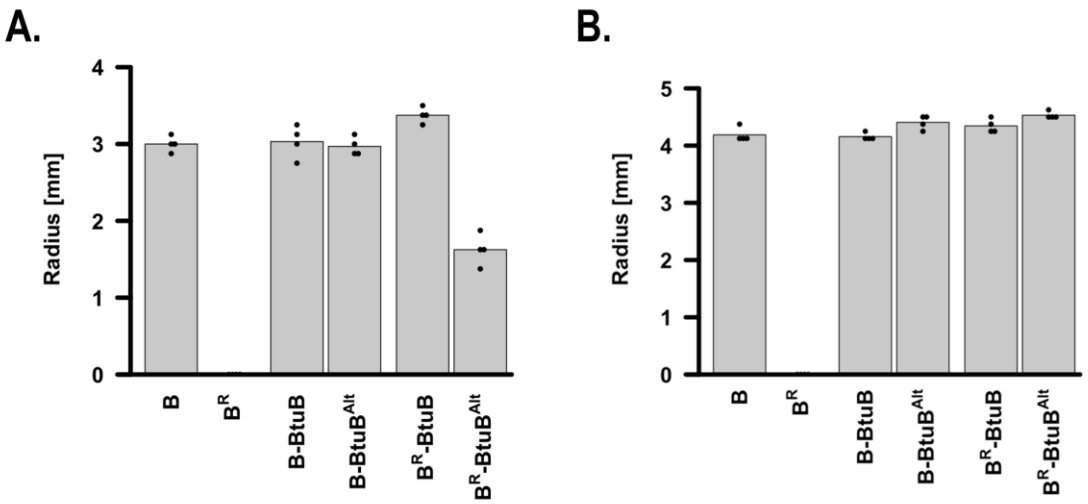

Fig. S25. An alternative *btuB* allele promotes partial resistance to colicin E4. In approximately 7% of *E. coli* genomes, the *btuB* gene is very divergent (see Fig. S24 and Dataset S3). We cloned one of these divergent alleles, $btuB^{Alt}$ from *E. coli* 96.0497, downstream the promoter of the BZB1011 *btuB* gene. We also cloned the BZB1011 *btuB* gene controlled by its own promoter. Both receptors were inserted at the Tn7 insertion site in the chromosome of the BZB1011 (B) and BZB1011 (*btuB*) (B^R) strains. A) A diluted suspension of each strain along with the parental strains (B and B^R) was spread onto the surface of 1.5% w/v LB agar plates using a sterile cotton swab. 10 mm wells were made in the plates and filled with 130 µl of normalized spent media from BZB1011 cells harboring pColE4. After 16 hours of incubation at 37°C, the zone of growth inhibition around the wells was measured. While complementation of B^R with the BZB1011 *btuB* receptor gene fully re-sensitizes this strain to colicin E4, $btuB^{Alt}$ promotes partial resistance to this toxin (p-value<0.05, two-sided t-test). B) The same experiment was performed with culture supernatant from BZB1011 cells harboring pColE2; in this case complementation with $btuB^{Alt}$ led to a strain fully sensitive to colicin E2 (p-value>0.05, two-sided t-test). We can conclude that the $BtuB^{Alt}$ receptor promotes partial resistance to a subset of colicins and could, therefore, benefit strains using provocation.

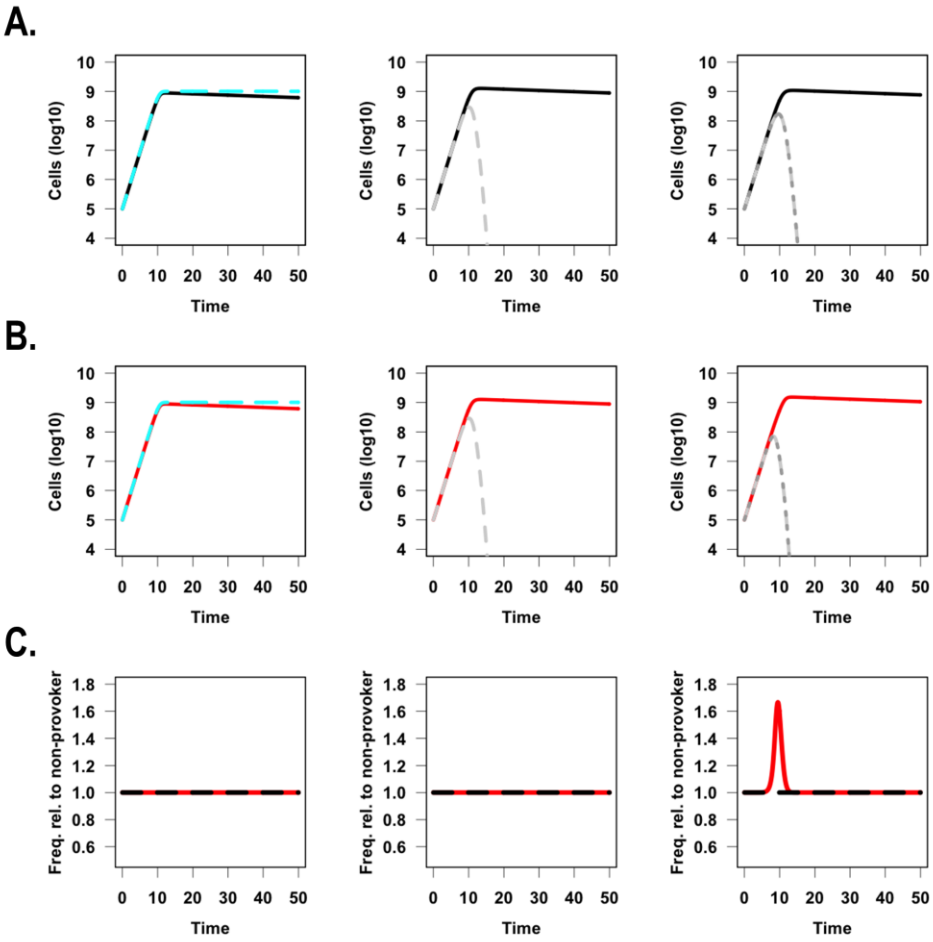

Fig. S26. Resistant aggression-provoking strains benefit in three-member colicinogenic communities compared to resistant non-provoking strains while they do equally well in other environments. The two first rows of graphs show the dynamics of modeled populations as a function of time in simulations where a resistant non-provoking-toxin producer (first row, in black) or a resistant provoking-toxin producer (second row, in red) compete with a resistant non-producer (first column, in cyan), a sensitive non-provoking toxin producer (second column, in light grey), or two sensitive non-provoking toxin producers (third column, in light and dark grey). The third row of graphs shows the frequency of the resistant provoker (red) and non-provoker (black) relative to a sensitive non-provoking strain in each competition scenario.

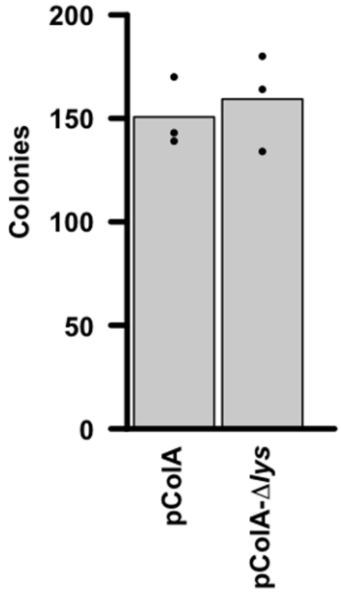

Fig. S27. A colicin with DNase activity kills target cells containing a colicin plasmid independently of their lysis gene. In our mathematical model, we assume that toxin molecules which get internalized by a target cell always kill it, irrespectively of whether they are capable of provocation or not. More specifically, if the toxin is a non-provoking one, the target cell will simply die, while if the toxin is a provoking one, the target cell will produce its own toxins prior to lysing. Here we prove that the release of DNase toxins does not provide additional benefits to the producing strain by killing target colicinogenic cells through the induction of their lysis gene which is controlled by SOS response. The scope of the assay was to show that the presence of a lysis gene does not influence the toxicity of colicin E2 on a colicin-A-producing strain. Briefly, we exposed normalized exponential cultures of BZB1011 cells harboring the pColA plasmid or a variant of it without the lysis gene, to spent medium from BZB1011 cells expressing colicin E2. After a two-hour incubation of the two strains in the presence of the DNase toxin, we plated the resulting suspensions and incubated them at 37°C for 16 hours. The difference in the viability of the two strains is not significant (p-value > 0.5, Student's t-test).

SUPPLEMENTARY INFORMATION TABLES

Table S1. Plasmids used in this study.

Name	Description	Source
pColA	Colicin A natural plasmid	(14)*
pColE1	Colicin E1 natural plasmid	(14)*
pColE2	Colicin E2 natural plasmid	(14)*
pColE4	Colicin E4 natural plasmid	(14)*
pColE7	Colicin E7 natural plasmid	(14)*
pColE8	Colicin E8 natural plasmid	(14)*
pUA66	pUA66 vector, promotorless GFP, Kan^R	This study
pUA66-P*colA*::*gfp*	GFP transcribed from *colA* promoter, pUA66	(15)
pGRG25	Plasmid encoding a Tn*7* transposon and arabinose-inducible *tnsABCD*; thermosensitive origin of replication pSC101, Amp^R	(16)
pUltraGFP-GM	Plasmid providing constitutive sfGFP expression from a strong synthetic Biofab promoter, p15A origin of replication, $Gent^R$	(17)
pUltraRFP-GM	Plasmid providing constitutive mRFP1 expression from a strong synthetic Biofab promoter, p15A origin of replication, $Gent^R$	(17)
pGRG25-P*max*::*gfp*	P*max::gfp* fragment from pUltraGFP-GM cloned within the Tn*7* of pGRG25; once the construct is inserted in the chromosome and the plasmid eliminated, the strain is labelled P*max*::*gfp*	(18)
pGRG25-P*max*::*rfp*	P*max::rfp* fragment from pUltraRFP-GM cloned within the Tn7 of pGRG25; once the construct is inserted in the chromosome and the plasmid eliminated, the strain is labelled P*max*::*rfp*	This study
pGRG25-P*max*::*rfp*-*btuB*	BZB1011 *btuB* gene controlled by its own promoter (P*btuB::btuB*) cloned within the Tn7 of pGRG25-P*max*::*rfp*; once the construct is inserted in the chromosome and the plasmid eliminated, the strain is labelled P*max*::*rfp* and expresses *btuB*	This study
pGRG25-P*max*::*rfp*-$btuB^{Alt}$	Alternative *btuB* allele ($btuB^{Alt}$) from *E. coli* 96.0497 controlled by the promoter of BZB1011 *btuB* (P*btuB::*$btuB^{Alt}$) cloned within the Tn7 of pGRG25-P*max*::*rfp*; once the construct is inserted in the chromosome and the plasmid eliminated, the strain is labelled P*max*::*rfp* and expresses *btuB*	This study
pColA-Cm	pColA with chloramphenicol resistance inserted downstream of the colicin A operon, Cam^R	(18)
pColE2-Cm	pColE2 with chloramphenicol resistance inserted downstream of the colicin E2 operon, Cam^R	(18)
pColA-Cm-Δlys	pColA-Cm with truncated lysis protein coding sequence (not including from codon 19 to TAA), Cam^R	This study
pColE2-Cm-Δ*tox*	pColE2-Cm with truncated toxin E2 protein coding sequence (267 nucleotides deleted from the toxic domain), Cam^R	This study
pColE2-Cm-Δ*opn*	pColE2-Cm with deletion of the entire E2 operon, Cam^R	This study

*Information on the origin of natural colicin plasmids used in this study can be found in (14)

Table S2. Bacterial strains used in this study.

Name	Description	Source
BZB1011	W3110, *gyrA*, Str^R	(20)
BZB1011 (*btuB*)	spontaneous *btuB* mutant of BZB1011 (gene disrupted by IS2)	This study

Table S3. Oligonucleotide primers for cloning used in this study.

Name	DNA sequence (5´-3´)
P1	AGGCGATCGGAGCTCCTTTCGCTAAGGATGATTTCTGG
P2	AGGGCGGCCGCTTAATTAAGAGCTCGAGTCAGTGAGCGAGGAAGC
P3	GCGGCCGCTCAGATGTCCAGATCTTGATGAATTC
P4	GCGGCCGCTCAGAAGGTGTAGCTGCCAGAC
P5	GCGGCCGCTCAGAAAGTATAGCTGCCAGAC
P6	TGCGGCAAGCAGCATGAT
P7	TAAAGGATCTTCTTGAGATCCTTTTACG
P8	CATGATCAATACTGTACATAAAACCACTGG
P9	GAAATCCTCTTTGACAAAAACAAAGC
P10	TTTACTCTCCTTATCTAATTTATCCTTAGCGTC
P11	TAAGGTAGGGAACGCTTTGAATTACATC
P12	GCCAACGTCGCATCTGGTTC
P13	CTATGGTAATACCGGAACG
P14	GAAGGTTATCGCTTCATTGC

LEGENDS FOR SUPPLEMENTARY INFORMATION DATASETS

Dataset S1. More than 30% of sequenced *E. coli* and related bacteria isolated from healthy individuals in the Human Microbiome Project encode colicins. 51 assembled reference genomes from bacteria of genus *Escherichia*, *Citrobacter* or *Klebsiella* were searched for the presence of colicin genes using blastp (9) on the predicted proteome (evalue < 0.01). Number of colicins per strain (first tab) and detailed results (second tab) are shown.

Dataset S2. In about 50% of human stool samples in which colicins are detected, two or more different colicins are found. Between 3 and 3.5 Gbases of reads extracted from each FijiCOMP individual stool microbiome database were searched for the presence of colicin-encoding genes using tblastn (9). The total number of colicin genes (at least three reads, more than 95% identity and 60 bp coverage, more than 15% of the colicin gene length) found within each of the 175 samples is shown.

Dataset S3. In approximately 0.7% and 7% of the NCBI *E. coli* genomes, the *btuB* gene is either absent or divergent, respectively. 4,016 *Escherichia coli* proteomes from the NCBI database were searched for homologs of the BtuB sequence using Hidden Markov Models. The table shows the number of BtuB homologs belonging to the core *E. coli* genome or divergent receptors (denoted by "Alt.") found in each genome, and a summary of the results.

SUPPLEMENTARY INFORMATION REFERENCES

1. Monod J (1942) *Recherches sur la croissance des cultures bacteriennes* (Paris: Herman).

2. Koch AL, Robinson JA, & Milliken GA (1998) *Mathematical modeling in microbial ecology* (New York: Chapman & Hall).

3. Majeed H, Lampert A, Ghazaryan L, & Gillor O (2013) The weak shall inherit: bacteriocin-mediated interactions in bacterial populations. *PloS One* 8(5):e63837.

4. Mitsui E & Mizuno D (1969) Stabilization of colicin E2 by bovine serum albumin. *J. Bacteriol.* 100(2):1136-1137.

5. Gordon DM & Riley MA (1999) A theoretical and empirical investigation of the invasion dynamics of colicinogeny. *Microbiology* 145 (Pt 3):655-661.

6. Soetaert K, Petzoldt T, & Setzer RW (2010) Solving differential equations in R: Package *deSolve*. *J. Stat. Softw.* 33(9):1-25.

7. Biernaskie JM, Gardner A, & West SA (2013) Multicoloured greenbeards, bacteriocin diversity and the rock-paper-scissors game. *J. Evol. Biol.* 26(10):2081-2094.

8. Kerr B, Riley MA, Feldman MW, & Bohannan BJ (2002) Local dispersal promotes biodiversity in a real-life game of rock-paper-scissors. *Nature* 418(6894):171-174.

9. Altschul SF, Gish W, Miller W, Myers EW, & Lipman DJ (1990) Basic local alignment search tool. *J. Mol. Biol.* 215(3):403-410.

10. Finn RD, *et al.* (2015) HMMER web server: 2015 update. *Nucleic Acids Res.* 43(W1):W30-38.

11. Edgar RC (2010) Search and clustering orders of magnitude faster than BLAST. *Bioinformatics* 26(19):2460-2461.

12. Price MN, Dehal PS, & Arkin AP (2010) FastTree 2 - Approximately maximum-likelihood trees for large alignments. *PloS One* 5(3):e9490.

13. Edgar RC (2004) MUSCLE: multiple sequence alignment with high accuracy and high throughput. *Nucleic Acids Res.* 32(5):1792-1797.

14. Ghazaryan L, Tonoyan L, Ashhab AA, Soares MI, & Gillor O (2014) The role of stress in colicin regulation. *Arch. Microbiol.* 196(11):753-764.

15. Kamensek S, Podlesek Z, Gillor O, & Zgur-Bertok D (2010) Genes regulated by the *Escherichia coli* SOS repressor LexA exhibit heterogeneous expression. *BMC Microbiol.* 10:283.

16. McKenzie GJ & Craig NL (2006) Fast, easy and efficient: site-specific insertion of transgenes into Enterobacterial chromosomes using Tn*7* without need for selection of the insertion event. *BMC Microbiol.* 6.

17. Mavridou DA, Gonzalez D, Clements A, & Foster KR (2016) The pUltra plasmid series: A robust and flexible tool for fluorescent labeling of Enterobacteria. *Plasmid* 87-88:65-71.

18. Mavridou DA, Gonzalez D, Kim W, West SA, & Foster KR (2018) Bacteria use collective behavior to generate diverse combat strategies. *Curr. Biol.* 28(3):345-355.

19. Roschanski N & Strauch E (2011) Assessment of the mobilizable vector plasmids pSUP202 and pSUP404.2 as genetic tools for the predatory bacterium *Bdellovibrio bacteriovorus*. *Curr. Microbiol.* 62(2):589-596.

20. Pugsley AP & Schwartz M (1983) A genetic approach to the study of mitomycin-induced lysis of *Escherichia coli* K-12 strains which produce colicin E2. *Mol. Gen. Genet.* 190(3):366-372.